

NOVEL DETECTION TECHNIQUES FOR VIABLE BUT NONCULTURABLE
VIBRIO VULNIFICUS CELLS IN RESPONSE TO ELEVATED SALINITY

by

Brandon McHenry

A Thesis Submitted to the Faculty of

The Charles E. Schmidt College of Science

In Partial Fulfillment of the Requirements for the Degree of

Master of Science

Florida Atlantic University

Boca Raton, FL

May 2019

Copyright 2019 by Brandon McHenry

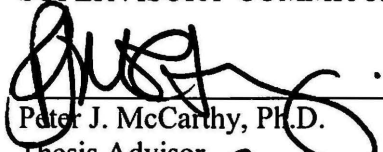
NOVEL DETECTION TECHNIQUES FOR VIABLE BUT NONCULTURABLE
VIBRIO VULNIFICUS CELLS IN RESPONSE TO ELEVATED SALINITY


by

Brandon McHenry

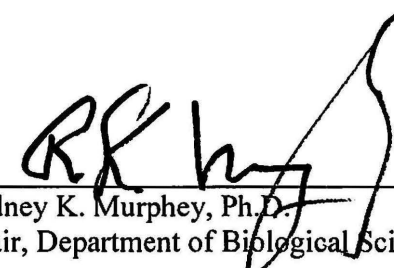
This thesis was prepared under the direction of the candidate's thesis advisor, Dr. Peter J. McCarthy, Department of Biology, and has been approved by all members of the supervisory committee. It was submitted to the faculty of the Charles E. Schmidt College of Science and was accepted in partial fulfillment of the requirements for the degree of Master of Science.


SUPERVISORY COMMITTEE:



Peter J. McCarthy, Ph.D.
Thesis Advisor


Esther Guzmán, Ph.D.


M. Dennis Hanisak, Ph.D.


Rodney K. Murphey, Ph.D.
Chair, Department of Biological Sciences


Ata Sarafedini, Ph.D.
Dean, Charles E. Schmidt College of Science


Khaled Sobhan, Ph.D.
Interim Dean, Graduate College

April 11, 2019
Date

ACKNOWLEDGMENTS

I would like to thank my thesis advisor, Dr. Peter J. McCarthy, and my committee members, Dr. Esther Guzmán and Dr. Dennis Hanisak, for their amazing support and guidance through this experience. I would also like to thank Dedra Harmody and Tara Pitts for providing me the skills to be successful in this process. A special thanks to Dr. Gabby Barbarite both for her expertise in *Vibrio* research and her public speaking and scientific communication skills. I would also like to acknowledge my lab mates, David Bradshaw, Carlie Perricone and Hunter Hines for help with statistical analysis, microbiological preparations and microscopy assistance. Lastly, I would like to extend my deepest gratitude to the Harbor Branch Foundation, the Link Foundation and Mission: Ocean Discovery for funding this research.

ABSTRACT

Author: Brandon G. McHenry
Title: Novel Detection Techniques for Viable But Nonculturable *Vibrio vulnificus* Cells in Response to Elevated Salinity
Institution: Florida Atlantic University
Thesis Advisor: Dr. Peter J. McCarthy
Degree: Master of Biological Sciences
Year: 2019

Vibrio vulnificus is a marine pathogen of human health concern, capable of causing potentially fatal wound infections in a select group of the population. Previous studies have indicated this species' strong negative correlation with salinity, not typically found above 30 ppt. This study assessed the ability of *V. vulnificus* to become Viable But Nonculturable in response to elevated salinity (35 ppt) as well as investigated novel methods for confirming their entrance into this state. Results showed a complete loss of culturability in both Environmental and Clinical strains of this bacterium by 9 days after inoculation. Using a High Content Imager, it was determined that these pathogens were not dying (< 10%) in response to the treatment and were partially becoming cocci (\approx 35%). This study indicates the importance of understanding the impact environmental parameters have on this human pathogen, and what it means for reliably detecting them.

DEDICATION

I would like to dedicate this manuscript to my family. My parents have always been my biggest supporters and have worked their lives to better mine and my brother's. They have always believed in me and told me that I could do whatever I set my mind to. They have helped shape me into the man that I am today, and for that I thank them.

NOVEL DETECTION TECHNIQUES FOR VIABLE BUT NONCULTURABLE
VIBRIO VULNIFICUS CELLS IN RESPONSE TO ELEVATED SALINITY

| | |
|---|----|
| LIST OF FIGURES | ix |
| 1 INTRODUCTION | 1 |
| 1.1 <i>Vibrio</i> Bacteria | 1 |
| 1.2 <i>Vibrio</i> and Human Health | 1 |
| 1.3 <i>Vibrio vulnificus</i> | 3 |
| 1.4 <i>Vibrio vulnificus</i> in the Environment | 5 |
| 1.5 <i>Vibrio vulnificus</i> and the Viable But Nonculturable State | 7 |
| 1.6 <i>Vibrio vulnificus</i> and the Indian River Lagoon | 10 |
| 1.7 Project Overview | 13 |
| 1.8 Hypotheses | 14 |
| 2 METHODS | 15 |
| 2.1 Culturing of Control Stocks | 15 |
| 2.2 Preparation of Cells | 15 |
| 2.3 Microcosm Set-up | 16 |
| 2.4 Microcosm Sampling | 16 |

| | | |
|------|---|----|
| 2.5 | Plate Count Analysis | 17 |
| 2.6 | Sample Preparation for High Content Imaging..... | 17 |
| 2.7 | Data Collection Using High Content Imaging | 18 |
| 2.8 | High Content Image Data Analysis..... | 21 |
| 2.9 | Image Selection for High Content Imagery Analysis | 26 |
| 2.10 | Statistical Analyses | 27 |
| 3 | RESULTS | 29 |
| 3.1 | Tracking Culturability of <i>Vibrio vulnificus</i> in Microcosms at Two Salinities... | 29 |
| 3.2 | <i>BacLight</i> Live/Dead Viability Assay Using the High Content Imager..... | 31 |
| 3.3 | Morphological Analysis Using the High Content Imager..... | 36 |
| 4 | DISCUSSION..... | 41 |
| 4.1 | Methods Development | 41 |
| 4.2 | <i>BacLight</i> Live/Dead Viability Assay Using the High Content Imager..... | 47 |
| 4.3 | Morphological Analysis Using the High Content Imager..... | 48 |
| 5 | CONCLUSIONS | 51 |
| | REFERENCES | 54 |

LIST OF FIGURES

| | |
|--|----|
| Figure 1 Depicts the custom journal created to partially automate the image collection process. The settings present in the “Configure Laser Autofocus” window are representative of what was used during the course of the experiment.... | 20 |
| Figure 2 Representative settings used to determine what constituted a true <i>V. vulnificus</i> cell and not debris in the image. | 22 |
| Figure 3 Representative settings used to determine what constituted live <i>V. vulnificus</i> cells. | 22 |
| Figure 4 Depicts representative settings used to determine what constituted dead <i>V. vulnificus</i> cells..... | 23 |
| Figure 5 Custom analysis created to analyze <i>V. vulnificus</i> cells by size and categorize them based on the categories of “Rods”, “Cocci” and “Transition”..... | 24 |
| Figure 6 Illustration of the “Auto-Find Blobs” filter designed to capture all objects that fall into the designated width measurements (min - 0.5 μm , max – 2.6 μm). | 24 |
| Figure 7 Illustration of the “Filter Mask” for all objects defined as a <i>V. vulnificus</i> cell. This filter captured objects between 0.5 and 2.6 μm long (largest distance across the cell, regardless of orientation) with a minimum intensity of 1000 and helped remove the space between the cells..... | 25 |
| Figure 8 Illustration of the “Filter Mask” for cocci. This filter captured objects between 0.5 and 1.1 μm long (largest distance across the cell, regardless of orientation). | 25 |

| | |
|--|----|
| Figure 9 Illustration of the “Filter Mask” for curved rods. This filter captured objects between 1.4 and 2.6 μm long (largest distance across the cell, regardless of orientation)..... | 26 |
| Figure 10 Illustration of two types of images discarded from analysis. The image on the left showcases a large obstruction, causing the image to be out of focus. The image on the right is blurry, causing distortion and inaccurate cell size measurements..... | 27 |
| Figure 11 Demonstration of an inaccurate analysis of an image. On the left is an image of several hundred <i>V. vulnificus</i> cells on Transmitted Light 25. The right shows the customs analysis for cell size counting several thousand cells. This analysis is not representative of the image shown on the left and was discarded. | 27 |
| Figure 12 Comparison of culturability over time for <i>V. vulnificus</i> Environmental strain (vcgE) in a control (11 ppt) and treatment (35 ppt) microcosm. Graph shows the averages of the duplicate plate counts among the three replicate trials with standard error. | 30 |
| Figure 13 Comparison of culturability over time for <i>V. vulnificus</i> Clinical strain (vcgC) in a control (11 ppt) and treatment (35 ppt) microcosm. Graph shows the averages of the duplicate plate counts among the three replicate trials with standard error. | 31 |
| Figure 14 Representative CHROMagar Vibrio plates. On the left is a plate illustrating the growth of a control population. The plate on the right shows the complete decline of culturability of <i>V. vulnificus</i> after 9 days in the treatment microcosm..... | 31 |

| | |
|--|----|
| Figure 15 Relative proportions of live, dead and unstained cells over a time series for <i>Vibrio vulnificus</i> Environmental strain (vcgE) in the control microcosm (11 ppt). ... | 33 |
| Figure 16 Relative proportions of live, dead and unstained cells over a time series for <i>Vibrio vulnificus</i> Environmental strain (vcgE) in the treatment microcosm (35 ppt). | 34 |
| Figure 17 Relative proportions of live, dead and unstained cells over a time series for <i>Vibrio vulnificus</i> Clinical strain (vcgC) in the control microcosm (11 ppt). | 34 |
| Figure 18 Relative proportions of live, dead and unstained cells over a time series for <i>Vibrio vulnificus</i> Clinical strain (vcgC) in the treatment microcosm (35 ppt). | 35 |
| Figure 19 Relative proportion of live <i>V. vulnificus</i> cells, shown in the left image, and dead cells, shown in the right image, for a representative control population at the end of the time series. | 35 |
| Figure 20 Relative proportion of live <i>V. vulnificus</i> cells, shown in the left image, and dead cells, shown in the right image, for a representative treatment population at the end of the time series. | 36 |
| Figure 21 Relative proportions of rods, cocci and transitional cells over a time series for <i>Vibrio vulnificus</i> Environmental strain (vcgE) in the control microcosm (11 ppt). | 38 |
| Figure 22 Relative proportions of rods, cocci and transitional cells over a time series for <i>Vibrio vulnificus</i> Environmental strain (vcgE) in the treatment microcosm (35 ppt). | 39 |
| Figure 23 Relative proportions of rods, cocci and transitional cells over a time series for <i>Vibrio vulnificus</i> Clinical strain (vcgC) in the control microcosm (11 ppt)..... | 39 |

Figure 24 Relative proportions of rods, cocci and transitional cells over a time series

for *Vibrio vulnificus* Clinical strain (vcgC) in the treatment microcosm (35 ppt)..... 40

Figure 25 Images showcasing the change in *V. vulnificus* cell shape and size over the

course of the time series. The image on the left illustrates a representative

population on the day of inoculation. The image in the middle shows the control

population at the end of the time series. The image on the right shows the

treatment population at the end of the experiment..... 40

1 INTRODUCTION

1.1 *Vibrio* Bacteria

Vibrio is a genus of marine bacteria that can be found in almost every environment around the world (Blackwell and Oliver 2008). These bacteria are characterized as slightly curved Gram-negative rods that are motile using a single polar flagellum (Drake et al 2007). *Vibrio* spp. are non spore-forming heterotrophic bacteria that are both aerobic and facultatively anaerobic (Farmer & Hickman-Brenner 2006). With the exception of *V. cholerae* and *V. mimicus*, which can persist in freshwater, these bacteria require at least some salt in order to grow (Griffitt and Grimes 2013).

The members of this genus are prominent nutrient cyclers in both deep sea and coastal marine environments and are even responsible for bioluminescence (Takemura et al 2014). However, certain species are known to cause infections in humans using toxins and genetic virulence factors (Oliver 2015). Out of over 100 species known around the world, 15 have been shown to be human pathogens; the three most prevalent being *V. cholerae*, *V. parahaemolyticus* and *V. vulnificus* (Blackwell and Oliver 2008).

1.2 *Vibrio* and Human Health

Collectively, bacteria from the genus *Vibrio* cause an estimated 80,000 illnesses, 500 hospitalizations and 100 deaths in the United States each year (Newtown et al 2012). However, Florida consistently reports the highest number of vibriosis cases each year, with a yearly average of 133 cases across the state (Weis et al 2011). This past year, there

were 42 documented cases and 9 deaths from one species, *V. vulnificus*, alone (Florida Department of Health). Unlike the remainder of the country, which reports predominantly seafood related illnesses, Florida is roughly equally divided between seafood sickness and wound related infections, 45% and 42% respectively (Weis et al 2011). This trend is likely due to the favorable environmental conditions found in the state of Florida as well as a large coastal population that takes part in many marine-related recreational activities and seafood harvest (Kildow 2008).

Vibriosis infections are seen most commonly in individuals who exhibit some form of a weakened immune system (Daniels 2011). Some of the most notable conditions that make individuals prone to infection are liver disorders, elevated iron levels and diabetes (Weis et al 2011). On average, vibriosis has three main clinical symptoms; gastroenteritis, making up approximately 51% of all cases, wound infections, 24% of cases, and primary septicemia, 17% of cases (Hlady and Klontz 1996). These infections can always be directly linked to the marine environment either through eating contaminated seafood or exposing a new or preexisting injury to waters containing *Vibrio* spp. (Weis et al 2011). Due to its prevalence and recognition as a nationally notifiable disease, vibriosis is monitored by the Center for Disease Control and Prevention as a subset of the Cholera and Other *Vibrio* Illness Surveillance (COVIS) initiative. Despite the monitoring of cases, *Vibrio* spp. are not held to any water quality standards and are not monitored by State Health Departments (Yamazaki and Esiobu 2012). Interestingly, certain states like Florida will post advisories for beach safety without any information regarding the possible *Vibrio* population present (Yamazaki and Esiobu 2012).

1.3 *Vibrio vulnificus*

Vibrio vulnificus makes up approximately 12% of the vibriosis cases in the United States each year; however, it poses the most serious health risk. The majority of all cases (94%) require patient hospitalization or medical treatment and can be fatal (28%) in under 72 hours (CDC 2015). Illnesses occurring in individuals with weakened immune systems are more severe and result in approximately 50% mortality. Symptoms usually manifest in the gastrointestinal tract as nausea or diarrhea, in a wound as a necrotizing skin lesion or in the bloodstream as a fever or septic shock (Weis et al 2011). This bacterium produces a polysaccharide capsule, which helps it evade detection by the human immune system, and extracellular toxins which break down host tissue (Daniels 2011). Infections that are caught in the first few hours are capable of being treated using third generation cephalosporins. However, those wound infections that are not treated immediately typically result in surgical amputation of the affected body part to prevent septicemia (Oliver 2005). In regards to demographics, an interesting trend arises showing that over 90% of all reported *V. vulnificus* cases are in men. This is likely due to elevated blood iron levels, low levels of estrogen and a higher probability that they would participate in activities that could potentially lead to exposure (Oliver 2015).

V. vulnificus makes up approximately 20% of the wound-related deaths and almost all (95%) of the seafood illness-related deaths in the United States (Oliver 2015). Wound infections are typically in response to becoming injured or exposing a pre-existing wound to the marine environment (Shaw et al 2015). However, not every *V. vulnificus* cell poses the same risk and are categorized based on various genetic characteristics which play into the virulence of the cell (Drake et al 2007). Of the three

known biotypes, strains from Biotype 1 are responsible for all of the infections in the United States and are also the most common around the world (Oliver 2015).

Vibrio vulnificus has a species-specific marker, the hemolysin/cytolysin gene (*vvha*), that is highly conserved in its genetic material and is used in molecular techniques to detect *V. vulnificus* regardless of biotype or virulence (Wright et al 1993). Strains of *V. vulnificus* Biotype 1 show wide genetic diversity and have thus been subcategorized by genotype. Initial classifications inferred virulence of *V. vulnificus* using 16S rRNA sequence polymorphisms to divide the population into two groups based on association with clinical infections (Nilsson et al 2003). Type A referred to non-clinical, or environmental strains, while Type B referred to clinical strains (Nilsson et al 2003). A newer and more widely used PCR-based assay is now utilized to distinguish strains based on the presence or absence of a *virulence correlated gene* (Warner and Oliver 2008a). This approach classified those isolates associated with environmental origin as E-type (*vcgE*) and those implicated in human infections as C-type (*vcgC*) (Rosche et al 2004). While the distribution of these two strains can vary widely in nature, environmental and seasonal factors can play a role in their proportions. In estuarine environments, it has been shown that the majority of *V. vulnificus* cells present are of the Environmental strain, meaning lower risk for recreators (Han et al 2009). However, the proportions change when focusing on the water column alone, where both the Clinical and Environmental strains are equally distributed (Warner and Oliver 2008b). Interestingly, warmer temperatures also seem to be implicated in increased proportions of Clinical strain *V. vulnificus* in the environment (Warner and Oliver 2008b).

1.4 *Vibrio vulnificus* in the Environment

Vibrio vulnificus is found worldwide in areas with warm waters and can be cultured from water, sediment, plankton, shellfish as well as finfish (Oliver et al 1982). This bacterium is a natural inhabitant of the environment and is not introduced by any form of anthropogenic pollution. Unlike fecal indicator bacteria, *V. vulnificus* does not have any correlation with standard water quality indicators and thus is not monitored by the state health departments (Hardwood et al 2004). Since many chemical and physical water parameters such as nitrogen and phosphorus levels, pH, dissolved oxygen and turbidity have minimal effect on the distribution and abundance of these pathogens, management and treatment options for human health are difficult (Blackwell and Oliver 2008). Two factors that do have profound effects on the ecology of *V. vulnificus* are temperature and salinity (Blackwell and Oliver 2008).

Of these two environmental factors the most influential in the occurrence of *V. vulnificus*, is temperature. This bacterium can typically be found between 7 and 36 °C but has its highest growth rate between 20 and 32 °C (Blackwell and Oliver 2008). Since this pathogen has a strong positive correlation with temperature, it exhibits seasonality around most of the globe, becoming most abundant between May and November when the water temperatures are the warmest (Oliver 1995). In addition, the clinical, or disease-causing strain, becomes significantly more abundant during the late summer and early fall, typically outnumbering the environmental strain (Warner and Oliver 2008a). As a result, both seafood sickness and wound infections see increased incidence during these times of the year. *Vibrio vulnificus* can typically be found in coastal environments around the United States; however, its abundance is significantly higher in areas with warmer water

temperatures (Johnson et al 2012). Additionally, regions that support year-round populations of this pathogen see the highest number of vibriosis cases; the Atlantic and Gulf coasts in particular, accounting for 43% of the nation's infections (CDC 2013).

Salinity tends to be the second factor most important in the distribution and abundance of *V. vulnificus* (Blackwell and Oliver 2008). While this bacterium does require some salt to grow, it exhibits a strong negative correlation with salinity (Motes et al 1998). Even though *V. vulnificus* has a relatively wide salinity tolerance between 5 and 25 ppt, its optimal salinity for growth has been shown to be 11.5 ppt (Jacobs et al 2010). From this information, it follows that dramatic changes in salinity should impact where these populations can be found in the environment. Natural events such as rainfall, or anthropogenic events such as freshwater releases, can reduce salinities in coastal environments where these pathogens are found. Areas that were once unfavorable for the growth of this bacterium due to salinities outside of its optimal range may now be accessible for colonization (Yamazaki and Esiobu 2012). It follows that these types of events can be significant predictors of the presence of this pathogen in recreational waters. Alternatively, elevated salinities may make certain environments inhospitable to *V. vulnificus*. One such example was a severe drought in North Carolina where the estuarine salinities remained above 30 ppt, above the optimal level for this species, for 2½ years (Froelich et al 2012). *Vibrio vulnificus* could not be recovered during this event, but after the salinities had returned to normal, the population recovered (Froelich et al 2012).

1.5 *Vibrio vulnificus* and the Viable But Nonculturable State

In addition to a lack of sufficient monitoring of *V. vulnificus* in recreational waters, these bacteria have been known to “disappear” from environments in which they are typically found (Oliver 1995). A field study conducted by Tilton and Ryan (1987) found that *V. vulnificus* could not be detected in water or oyster samples collected from Boston Harbor, Maine from November to May. However, once the water warmed during the summer and fall months, these bacteria could be cultured from the oyster samples (Tilton and Ryan 1987). Oliver (1995) noticed a similar trend occurring during the winter months in North Carolina where *V. vulnificus* could not be cultured. After much research, this phenomenon was understood to be a survival mechanism by *V. vulnificus* to persist in the environment during periods of thermal stress. Instead of the population dying off during the winter months and being recolonized when the water warmed, it was discovered that these bacteria were able to overwinter (Oliver et al 1995).

Vibrio vulnificus is one of over 60 species that are able to become Viable But Nonculturable (VBNC) (Oliver 2005). When bacteria become VBNC, it is typically in response to some form of unfavorable environmental condition that allows them to persist until conditions become favorable (Oliver 1995). This form of dormancy response is most recognizable by a loss of culturability of these bacteria using standard bacteriological media (Oliver 1995). Cells that enter the VBNC state go through several dramatic changes. Major declines in protein, RNA and DNA synthesis happen very rapidly (<15 min) when environmental stressors occur (Oliver 1995). Potential changes to the chromosome of the bacteria may also occur as DNA-binding proteins are thought to be involved in the VBNC response (Oliver 1995). Significant decreases in nutrient

transport, metabolic activity, macromolecular synthesis and respiration rates have also been documented (Oliver 2009). A change in the structure of the cell wall takes place with changes in membrane fatty acid composition, a dramatic increase in DAP-DAP crosslinking, mucopeptides, and the average length of glycan strands (Oliver 2009). Despite these responses, VBNC cells do not stop all biosynthesis. Various shock proteins, such as cold shock proteins, and ATP levels remain high in cells that have become VBNC (Oliver 2005). For *V. vulnificus* in particular, a morphological change occurs, where standard 3 μm curved rods will transition into 0.6 μm cocci when the cell has become fully VBNC (Oliver 2009).

The VBNC phenomenon has been studied extensively for *V. vulnificus* in regards to thermal stress. A study conducted by Oliver et al (1995) in North Carolina attempted to capture the shift of *V. vulnificus* into the VBNC state during winter months in estuarine waters. Cells were grown to approximately 10^7 CFU/mL and inoculated into 0.2 μm polycarbonate membrane diffusion chambers, which allow water to pass through but not *V. vulnificus* cells (Oliver et al 1995). Diffusion chambers were placed into estuarine waters between 10 and 15 °C 20 cm below the surface. Samples were taken from diffusion chambers periodically and plated onto chromogenic Tn agar to count species specific colonies. Acridine Orange direct cell counts (AODC) and direct viable counts (DVC), done using the Kogure method, were also performed (Oliver et al 1995). While the culturable population of *V. vulnificus* had disappeared by day 14, the AODC and DVC assays showed approximately 10^7 cells/mL and 10^4 cells/mL respectively (Oliver et al 1995). To show that *V. vulnificus* could also be resuscitated after becoming VBNC, cells held dormant for at least 7 days from a lab experiment were placed into the same

membrane diffusion chambers at the same site during the month of November when the water temperature was 22 °C. The population of VBNC cells had regained complete culturability by the 4th day in the warmer water (Oliver et al 1995).

A second study designed to demonstrate the ability of *V. vulnificus* to become VBNC in response to reduced temperatures was conducted by Oliver and Whitesides (1996) in a laboratory setting. Clinical and environmental strains of *V. vulnificus* were grown in Heart Infusion (HI) broth at 37 °C and inoculated at a density of 10⁶ cells/mL into a microcosm incubated at 5 °C (Oliver and Whitesides 1996). After 4 days, the population of *V. vulnificus* was no longer culturable, but using AODC and DVC assays, approximately 10⁸ cells/mL were present and 10⁵ cells/mL were viable (Oliver and Whitesides 1996). Microcosms were then filtered through 0.2 µm Nucleopore membranes to remove any potentially culturable cells. Cells were then incubated at 22 °C and regained complete culturability after 10 hours (Oliver and Whitesides 1996).

Research has also shown that VBNC *V. vulnificus* cells can still retain their virulence and even resuscitate in vivo (Oliver and Bockian 1995). *Vibrio vulnificus* cells were induced into the VBNC state using 5 °C microcosms and held for 3 days after complete loss of culturability. VBNC cells (10⁵ cells/mL with culturability of <0.04 CFU/mL), were inoculated into an iron overloaded mouse (Oliver and Bockian 1995); the mouse typically died within 24 hours, indicating that VBNC *V. vulnificus* cells retained their virulence and were still capable of causing infection (Oliver and Bockian 1995). Furthermore, culturable *V. vulnificus* cells, confirmed by PCR, were recovered from the peritoneal cavity and heart, indicating that this pathogen reverted to the culturable state in vivo (Oliver and Bockian 1995).

Despite the amount of information available on *V. vulnificus* and its response to cold temperatures, there is little published research on how this pathogen deals with salinities outside of its optimal range. A study by Jones et al (2007) inoculated *V. vulnificus* cells into membrane diffusion chambers and placed them in estuarine waters at 21 ppt and 31 ppt, at 26.4 °C and 24 °C respectively, for 48 hours. No significant change in culturability was noticed after 48 hours at either moderate or high salinity (Jones et al 2007). The high-salinity treatment was continued for an additional 28 days; the culturable population did decline slightly, from 10^7 CFU/mL to 10^5 CFU/mL, however the cells did not become VBNC (Jones et al 2007). Another study conducted by Nowakowska and Oliver (2013) showed that 99.99% of the *V. vulnificus* population incubated in 290 ppt ASW for 120 min became VBNC in response to this stressor.

As these studies show, *V. vulnificus* cells can become VBNC in response to decreased water temperature, and to a lesser extent, elevated salinity. While in this state, these cells remain alive and can be detected using a mix of cell permeable and cell impermeable nucleotide dyes, such as the *BacLight* Live/Dead Viability Assay (Oliver 2009). Despite this, their inability to be cultured using standard bacteriological media presents a challenge to monitoring these important human pathogens in recreational areas with environmental parameters outside the typical tolerance range of this species.

1.6 *Vibrio vulnificus* and the Indian River Lagoon

The Indian River Lagoon (IRL) is an estuary of national significance that spans 156 miles and makes up approximately 40% of the east coast of Florida. The IRL spans 6 counties and in 2014 had a population of approximately 1.7 million people (Lapointe et al 2015). The Indian River Lagoon is made up of three water bodies, the Mosquito Lagoon,

the Banana River and the Indian River, that span 566,560 hectares (SJWMD 2007).

Together, the IRL is one of the most biologically diverse and productive estuaries in the Northern Hemisphere. Since parts of the IRL can be found in both the temperate and subtropical climate zones, the range of temperatures allows over 2000 species of plants and 2000 species of animals to thrive in the lagoon watershed. In particular, over 700 species of fish are known to utilize the IRL for part or all of their life histories (Gilmore et al 1981). In (2016) the East Central Florida Economic Planning Council updated the annual economic impact of the Indian River Lagoon to the state of Florida. This value was in excess of \$7.8 billion with aerospace and tourism as the top two industries. Recreational uses of the lagoon include fishing (38%), swimming and wading (20%) and boating (18%) (Lapointe et al 2015).

The IRL is a highly dynamic body of water with varying salinities that can be highly impacted by freshwater drainage canals, runoff, precipitation and tidal fluxes (Smith 1993). On average, the IRL receives 150 cm of rainfall over the course of a year, with the majority falling between the months of May and November (Martin et al 2006). In addition, there are five main inlets that flush the IRL with Atlantic Ocean water, with 50% turnover rates that are between one week in the southern IRL and just under a year in the northern IRL (Smith 1993). Coupled with many anthropogenic stressors such as urbanization, changes with hydrology and freshwater releases, the Indian River Lagoon is an environment that experiences fluctuations that affect populations of *V. vulnificus*.

Despite this, the IRL shares many characteristics with other *Vibrio* outbreak areas around the globe including a large recreating population, host species and ideal environmental conditions (Buck 1990; Tao et al 2012). Across the six counties that make

up the Indian River Lagoon, this region accounts for approximately 20% of the state's vibriosis cases (www.FloridaCHARTS.com). Over the last 30 years, the number of documented vibriosis cases have more than doubled in the IRL region. Prior to 2016, there have been no systemic monitoring studies looking at the abundance and distribution of pathogenic *Vibrio* species in the Indian River Lagoon.

The first and only study to document the occurrence of pathogenic *Vibrio* spp. in the IRL was a Ph.D. dissertation at Florida Atlantic University's Harbor Branch (Barbarite 2016). This study tested estuarine fish, water, sediment and oysters for three major human pathogens, *V. parahaemolyticus*, *V. vulnificus*, and *V. cholerae*, throughout the IRL with a focus on human health. It was found that these bacteria were permanent members of the microbial community in the IRL due to the year-round warm climate (Barbarite 2016). However, seasonality was still exhibited, with peaks in abundance between the months of August and October when the water was the warmest and there were the highest amounts of rainfall (Barbarite 2016). Additionally, these bacteria were found in highest abundance near the base of freshwater drainage canals further solidifying their strong negative correlation with salinity (Barbarite 2016). Conversely, sediment samples taken from the beach, Pepper Park, Fort Pierce FL, never yielded any culturable *Vibrio* cells for all 12 months of the year (Barbarite 2016). In addition, a model study was conducted that determined that even in a month with water temperature around 30 °C, *V. vulnificus* could not be recovered from water or fish samples taken from an environment where the salinity was above 33 ppt (Barbarite 2016). This data may suggest the shift of *V. vulnificus* into the VBNC state as a result of elevated salinity.

1.7 Project Overview

This research project was designed to track the culturability of *Vibrio vulnificus*, clinical (*vcgC*) and environmental (*vcgE*) strains, over a time series in two different salinity microcosms. A control microcosm was held at 11 ppt, which is the optimal salinity for *V. vulnificus*, and a treatment microcosm at 35 ppt, which is far outside the optimal salinity range for this species and representative of coastal oceans and high salinity areas in the IRL. Culturable cells were enumerated daily using a *Vibrio* specific chromogenic medium (CHROMagar *Vibrio*) in which *V. vulnificus* colonies grow a teal color. Populations were tracked until the number of CFU/mL fell below 10^1 . A concurrent experiment will be conducted by taking daily samples to check for viability using the *BacLight* Live/Dead Viability Assay. Samples were enumerated using the Molecular Devices ImageXpress Micro XLS High Content Imager using a 100x oil-immersion objective and scored for viability as well as size and shape analysis. The target questions of this project were:

- Will elevated salinity (35 ppt) induce the VBNC state in *V. vulnificus*?
- Are standard cultivation techniques reliable in monitoring for *V. vulnificus* above its salinity tolerance range?
- Does *V. vulnificus* exhibit a full morphological shift in cell shape and size as it loses culturability?
- Do environmental and clinical strains respond differently to osmotic stress?

1.8 Hypotheses

H₁: *Vibrio vulnificus* will become Viable But Nonculturable when incubated in elevated salinity (35 ppt).

H₂: Standard cultivation techniques will not be a reliable means of determining the presence of *V. vulnificus* in salinities above its tolerance range.

H₃: *Vibrio vulnificus* will shift completely from 3 µm curved rods to 0.6 µm cocci.

H₄: The environmental (*vcgE*) strain of *V. vulnificus* will be more resilient to osmotic stress than the clinical (*vcgC*) strain.

2 METHODS

2.1 Culturing of Control Stocks

Control stocks of *Vibrio vulnificus*, environmental and clinical strains, were obtained from a previous Ph.D. project at FAU Harbor Branch (Barbarite 2016) focusing on pathogenic *Vibrio* species. These controls were verified using PCR for both species and virulence type (Warner and Oliver 2008). Ten controls for each virulence type were stored frozen at -80 °C to ensure the same stock was used throughout the project. One vial each of *V. vulnificus* clinical and environmental strains were thawed and cultured in 10 mL Heart Infusion broth overnight in a shaker at 35 °C and 210 rpm for this experiment. The verified stocks were subcultured onto CHROMagar *Vibrio* grown at 37 °C and stored for up to a week at 25 °C.

2.2 Preparation of Cells

Two overnight cultures of *V. vulnificus*, clinical and environmental strains, were each grown in 10mL of Heart Infusion broth at 35 °C with shaking at 210 rpm. The cultures were harvested and washed twice by centrifugation, (1,863xg, 30 minutes) in Phosphate Buffered Saline (PBS; 8 g NaCl, 0.2 g KCl, 1.44 g Na₂HPO₄, 0.24 g KH₂PO₄, 1 L DI water). After washing, 1 mL of culture was diluted into 9 mL of PBS, optical density was determined (610 nm) and added to one of four experimental microcosms.

2.3 Microcosm Set-up

Ocean water (40 ppt) was collected from the Fort Pierce Inlet, Florida (27°47'11.58'' N, 80°28'78.72'' W) at high tide using a 20 L plastic polypin. The water was filter sterilized using a 0.22 µm cellulose acetate membrane (Corning # 430517). Filter-sterilized ocean water was transferred into a second ethanol-sterilized 20 L polypin for storage during the experiment. Duplicate microcosms, for clinical and environmental strains, respectively, were established in 1 L sterile glass bottles. The ocean water for the control microcosms was diluted with sterilized deionized water to 11 ppt, chosen because this is the optimal salinity for *V. vulnificus* (Jacobs et al 2010); the experimental microcosms were each diluted to 35 ppt, chosen because previous research in the area never recovered culturable cells from water or sediment with salinity this high. All microcosms were prepared with 495 mL water. Salinities were confirmed using a refractometer calibrated using reverse osmosis deionized water for a 0 ppt standard. Washed *Vibrio vulnificus* (5 mL per microcosm), clinical and environmental strain, was added to the appropriate microcosm to achieve a cell density of 10^7 cells/mL. The microcosms were held at 25 °C with shaking at 120 rpm for the duration of the time trial experiments.

2.4 Microcosm Sampling

Each microcosm was sampled immediately after inoculation at the start of the experiment, and once every 24 hours until the treatment population showed no culturable cells.

2.5 Plate Count Analysis

A 10-fold dilution series, in duplicate, from 10^{-1} to 10^{-6} was made in sterile PBS, by adding 500 μL of sample to 4.5 mL PBS. Each dilution was vortexed for 10 seconds to ensure the sample was homogenous. A volume of 100 μL was direct plated in duplicate from each dilution onto CHROMagar *Vibrio* growth medium (CHROMagar, Paris, France). Plates were incubated at 37 °C overnight. The number of visible colonies were counted for each dilution and calculated as the number of colony forming units (CFU) per mL per microcosm.

2.6 Sample Preparation for High Content Imaging

A volume of 1 mL from each microcosm was taken daily and stained using the BacLight Live/Dead Viability Assay that relies on cell permeability of two nucleic acid stains. Aliquots of SYTO 9 nucleic acid stain (excitation 485 nm, emission 498 nm) and propidium iodide non-permeable nucleic stain (excitation 535 nm, emission 617 nm) were mixed in equal proportions, 1.5 μL of each dye, prior to the beginning of the experiment to ensure the fluorescent intensity remained the same throughout the duration of the time trials. A 3 μL aliquot of premixed dye was added to each 1 mL sample and vortexed at maximum speed for 10 s. Samples were left covered in complete darkness for 25 min to allow the dyes to bind to the DNA. The samples were vortexed again at maximum speed for 10 s to resuspend the cells. To each 1 mL sample glutaraldehyde was added to a final concentration of 4% for fixation and vortexed at maximum speed for 10 s. Samples were incubated in darkness for an additional 5 min to allow for complete fixation. A volume of 100 μL from each sample was plated in duplicate into a 384-well glass bottom optical plate (Nunc # 240074). Samples were organized in the 384-well

plate so that each column represented a single day of the time trial and each set of two rows corresponded to a duplicate from each microcosm (totaling 8 rows of samples per run). The stained and fixed samples were centrifuged, at 3000 rpm for 15 min, daily in the 384-well plate to adhere the cells to the bottom of the glass. The plate was wrapped entirely in parafilm and aluminum foil and stored in complete darkness at 4 °C each day until it was analyzed using High Content Imaging.

2.7 Data Collection Using High Content Imaging

Prior to imaging, the Nunc 384-well optical glass plate containing stained and fixed samples was allowed to come to room temperature in complete darkness. Samples were then read using the Molecular Devices ImageXpress Micro XLS High Content Imager (HCI). All images were taken using a Nikon CFI Plan Fluor 100x Oil Immersion Objective and enough Cargille type B immersion oil to cover the inverted objective. The samples were imaged using three settings; FITC (475/34 nm), Texas Red (560/32 nm) and Transmitted Light 25 (25% of maximum white light). The plate layout consisted of 8 rows, each corresponding to a single duplicate from each of the four microcosms, and between 7 and 10 columns depending on the experimental replicate, each representing a single time point. Within each well, 9 equally spaced fields were chosen for imaging to gain a more representative view of the cells within each sample. No more than 10 individual wells in a row were imaged at one time to prevent the objective from running out of immersion oil.

This was the first time that the HCI had been used to image bacterial cells at 100x magnification and it became evident that this was not a standard protocol for the manufacturer. This resulted in many modifications to standard protocols being made

(Figure 1). Due to the small working distance between the 100x objective and the 384-well plate, the HCI cannot perform an autofocus protocol. The manual focus distance of the sample must be entered into the journal at the beginning of each run so that the objective does not contact the bottom of the glass plate and risk damage. A secondary safety threshold, of approximately 50 μm , for objective distance must also be entered each run to keep the objective from either coming out of the oil or pushing the plate up out of position. An offset value of 10 μm was added to the journal to allow the objective to compensate for small variations in the bottom of the glass while it was changing the focus in between sites. A secondary offset value of 0.7 μm was added to make up for the minor difference in focus between the fluorescent wavelengths, FITC and Texas Red, and the Transmitted Light 25. To accommodate for the different orientation of *V. vulnificus* cells, which is exaggerated at 100x magnification, a Z-stack of 8 images was taken above and below the main focus height in 0.1 μm intervals to help increase the resolution of the image. Finally, a background flattening protocol was added to reduce extraneous shadows in the brightfield images to help with post-processing analysis.

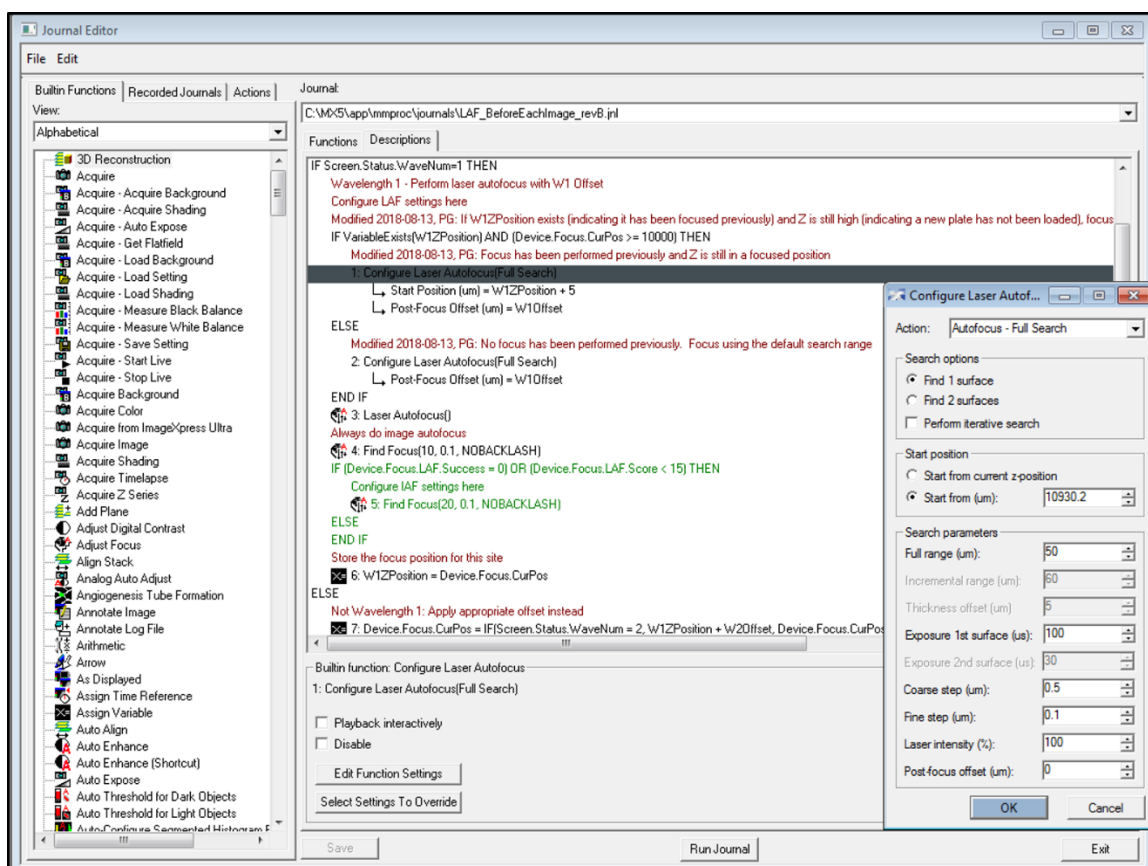


Figure 1 Depicts the custom journal created to partially automate the image collection process. The settings present in the “Configure Laser Autofocus” window are representative of what was used during the course of the experiment.

The images were first brought into focus manually using the MetaXpress software (version 5.3.0.5). Each row of wells was run using an automated image collection protocol with the modified journal. At the end of imaging a single row of samples, the plate would be removed from the HCI, and the glass as well as the 100x objective were wiped with lens cleaner to remove oil residue before running the next row of wells. The values specified in the modifications above had to be redetermined and entered at the start of running each new row of samples. Once the images were collected for the entire experiment, the data was transferred to a secondary computer for analysis.

2.8 High Content Image Data Analysis

Images collected from the Molecular Devices ImageXpress Micro XLS High Content Imager were analyzed using the MetaXpress Software package (version 5.3.0.5). Images taken under the fluorescent wavelengths, FITC and Texas Red, were analyzed using the software's pre-installed "multi-wavelength analysis". This analysis measures the fluorescence intensity of each individual cell for the chosen wavelengths and categorizes it as a positive or negative in comparison to overall background intensity. The brightfield, or Transmitted Light 25, wavelength acted as the positive control for the program to determine what it recorded as a true *V. vulnificus* cell and what was potential debris (Figure 2). The threshold range was set between 0.5 μm and 2.5 μm across with a minimum intensity of 1000 over background levels. Any object that did not fit into these parameters was not counted as a cell and would not register in the fluorescent channels, preventing extraneous dye particles from being measured. The FITC (Figure 3) and Texas Red (Figure 4) channels had the same threshold range from 0.5 μm to 2.5 μm , but each had intensity thresholds of 150.

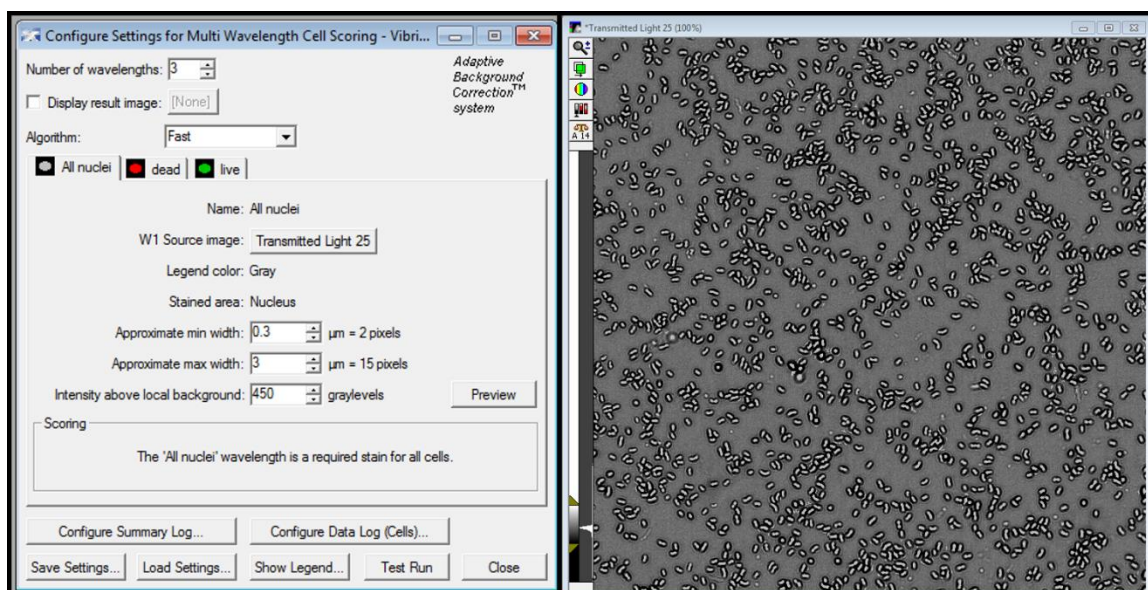


Figure 2 Representative settings used to determine what constituted a true *V. vulnificus* cell and not debris in the image.

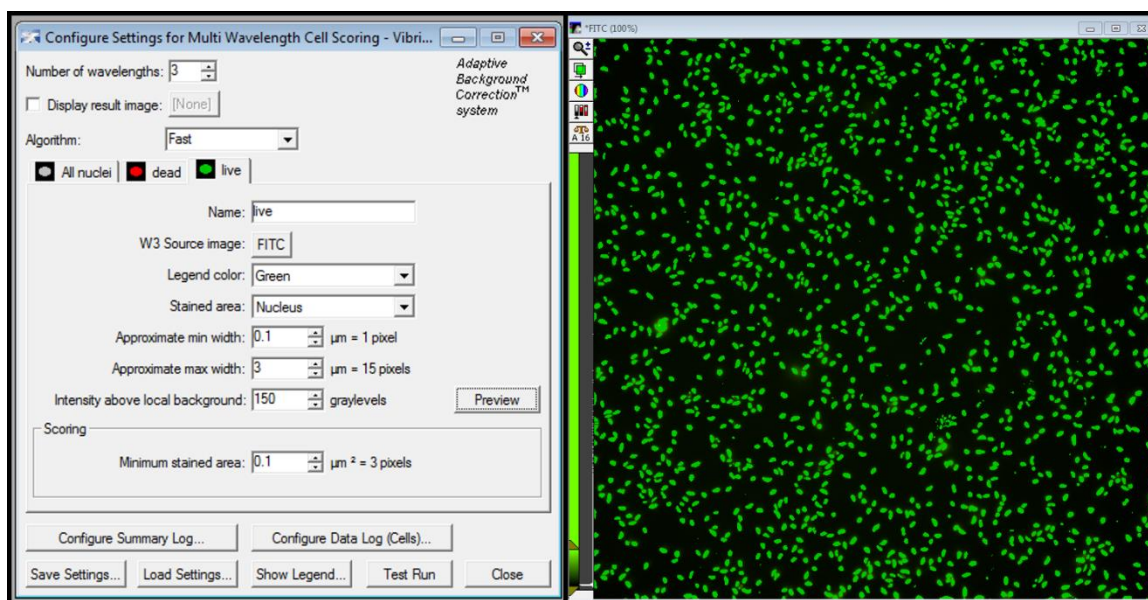


Figure 3 Representative settings used to determine what constituted live *V. vulnificus* cells.

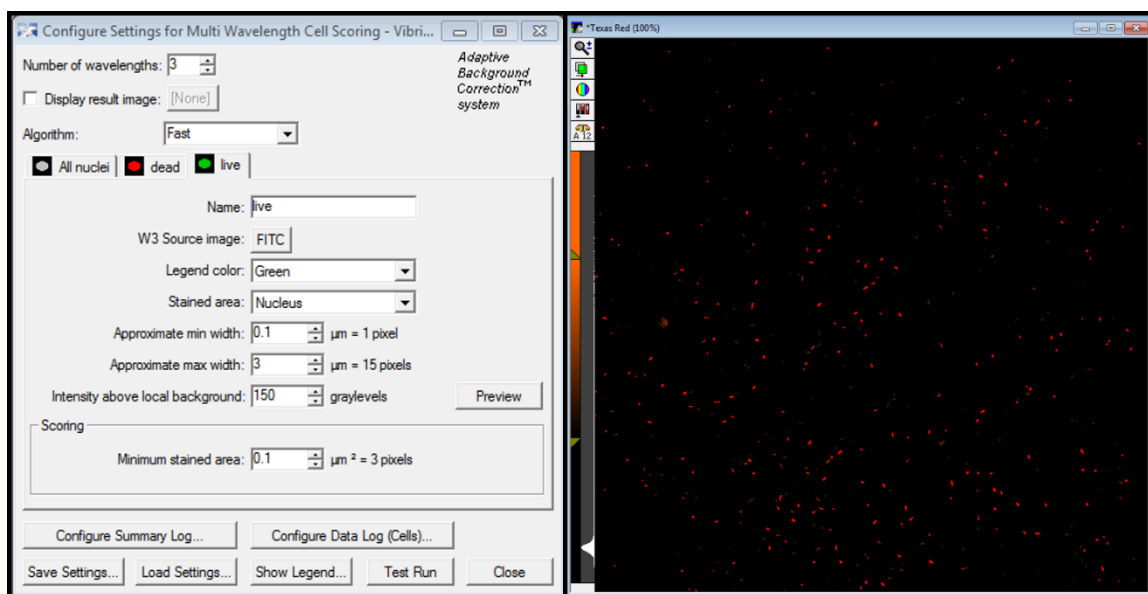


Figure 4 Depicts representative settings used to determine what constituted dead *V. vulnificus* cells

To measure the approximate shape of the *V. vulnificus* cells, a custom analysis module was created consisting of several steps (Figure 5). First, a series of smoothing filters were applied to help remove any additional background noise as well as smooth and refine the edges of the cells. Next, a preliminary search to mark cells was added, known as “auto-find blobs”, which used a horizontal width measurement of 0.5 to 2.5 μm (Figure 6). Subsequent filters (Figure 7) were added using length, a measure of the largest distance across a given cell in any direction, to define the two shape categories for this experiment. The “Cocci” filter marked all cells that were within the range of 0.5 to 1.1 μm in length and had an intensity above background levels of at least 1000 to differentiate from small bright spots in the background of the image (Figure 8). A second “Rod” category was created using a length measurement from 1.6 to 2.5 μm with an intensity above background levels of at least 1000 (Figure 9). Finally, a “simple threshold” was added to allow the machine to report individual cell counts for each of the three measured categories, “Filtered objects”, “Rods” and “Cocci”. The difference

between the number of cells in each of these three measurements resulted in the final category called “Transition”.

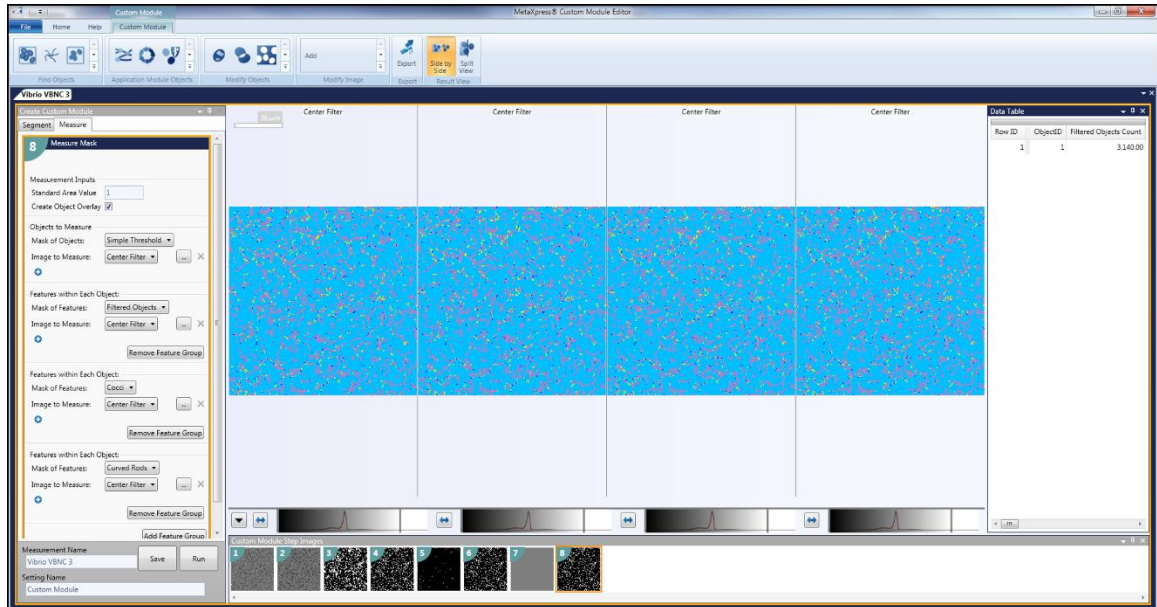


Figure 5 Custom analysis created to analyze *V. vulnificus* cells by size and categorize them based on the categories of “Rods”, “Cocci” and “Transition”.

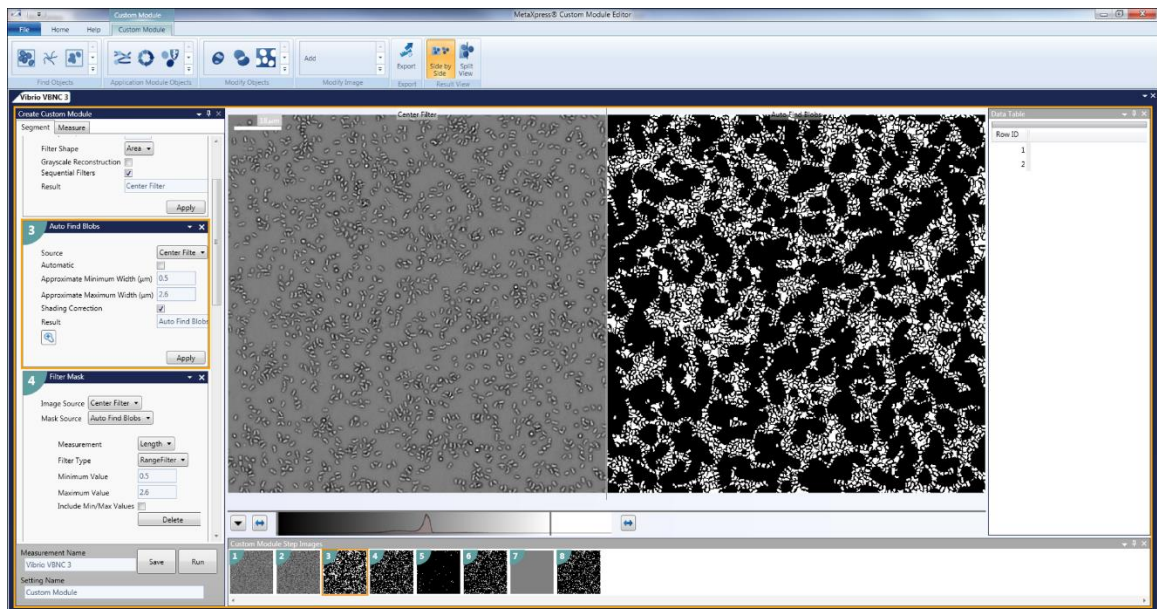


Figure 6 Illustration of the “Auto-Find Blobs” filter designed to capture all objects that fall into the designated width measurements (min - 0.5 μm , max – 2.6 μm).

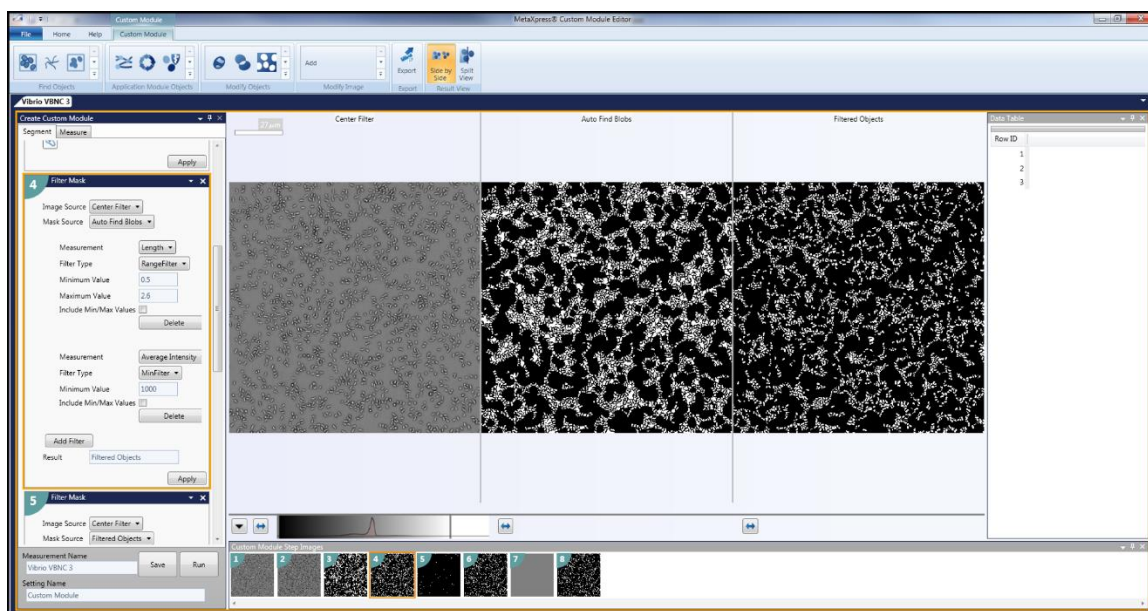


Figure 7 Illustration of the “Filter Mask” for all objects defined as a *V. vulnificus* cell. This filter captured objects between 0.5 and 2.6 μm long (largest distance across the cell, regardless of orientation) with a minimum intensity of 1000 and helped remove the space between the cells.

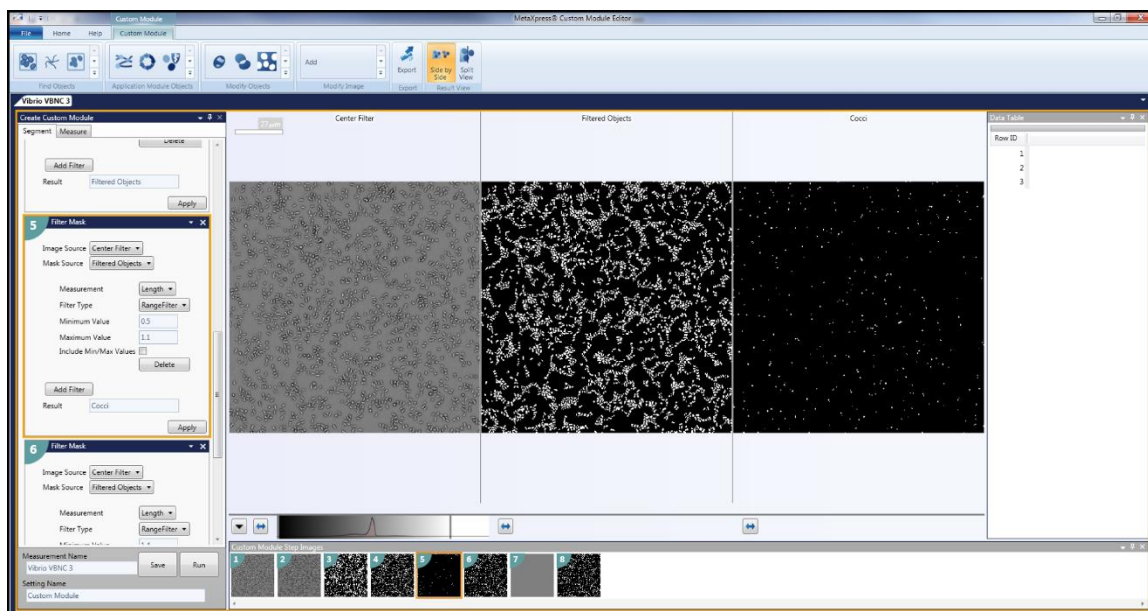


Figure 8 Illustration of the “Filter Mask” for cocci. This filter captured objects between 0.5 and 1.1 μm long (largest distance across the cell, regardless of orientation).

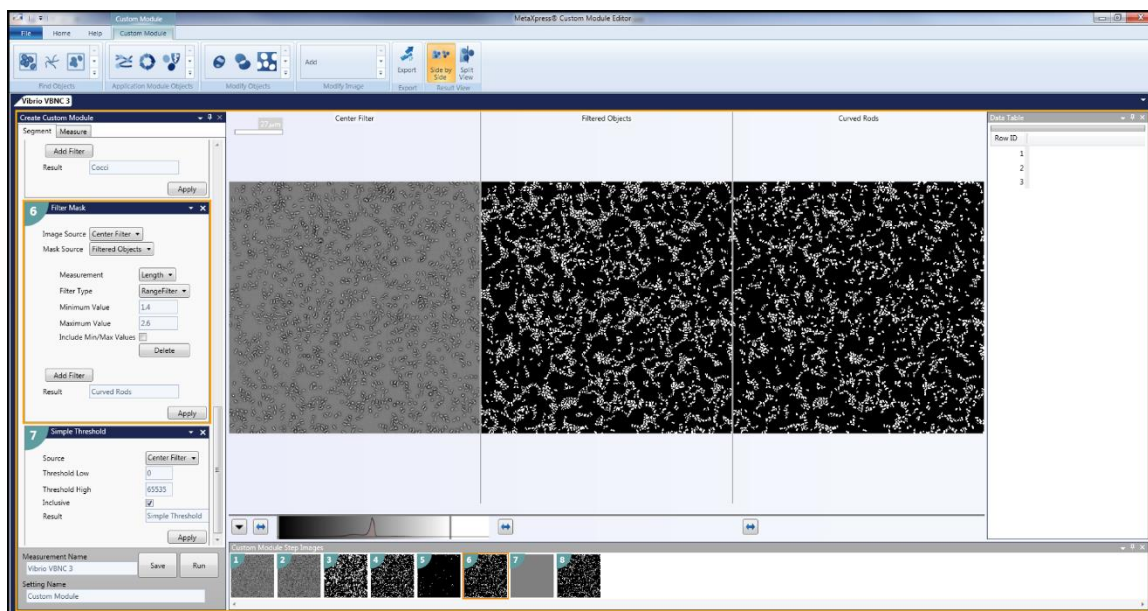


Figure 9 Illustration of the “Filter Mask” for curved rods. This filter captured objects between 1.4 and 2.6 μm long (largest distance across the cell, regardless of orientation).

2.9 Image Selection for High Content Imagery Analysis

Each image collected by the HCI was assessed before being analyzed. Any image that was out of focus was discarded and the results omitted. Additionally, any image that contained debris or other obstruction was not used (Figure 10). Finally, images with analyses not representative of the population present (counting 4,000 cells when only 200 are present) were also discarded (Figure 11).

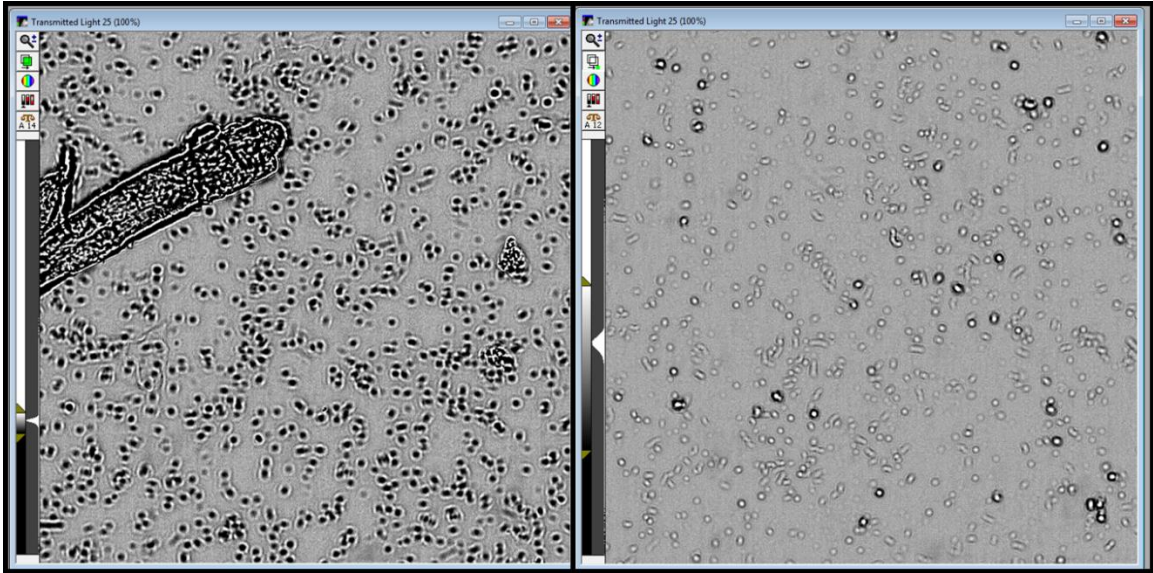


Figure 10 Illustration of two types of images discarded from analysis. The image on the left showcases a large obstruction, causing the image to be out of focus. The image on the right is blurry, causing distortion and inaccurate cell size measurements.

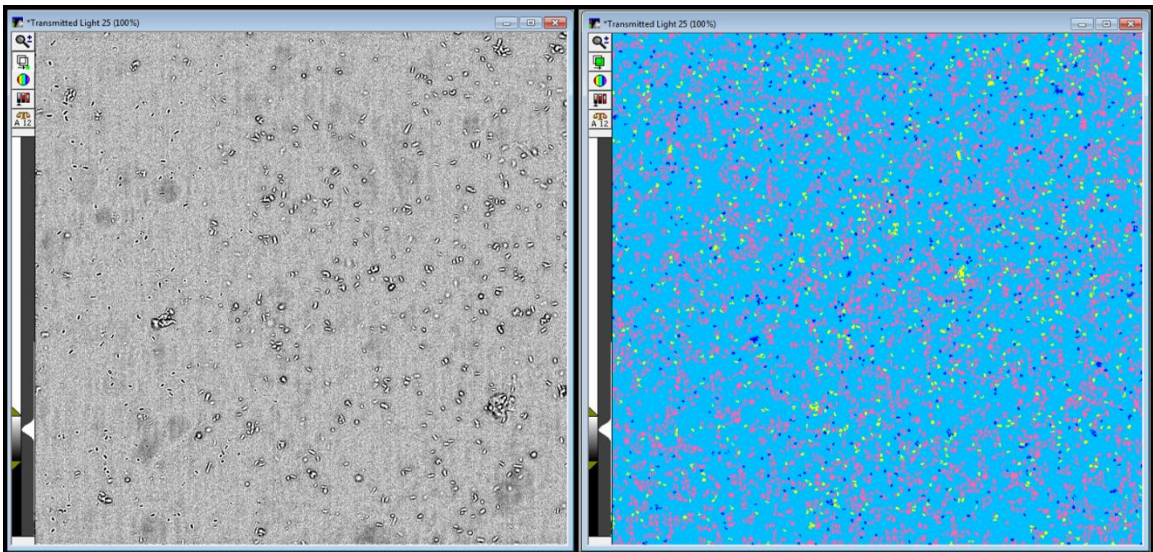


Figure 11 Demonstration of an inaccurate analysis of an image. On the left is an image of several hundred *V. vulnificus* cells on Transmitted Light 25. The right shows the custom analysis for cell size counting several thousand cells. This analysis is not representative of the image shown on the left and was discarded.

2.10 Statistical Analyses

Shapiro-Wilkes tests were used to determine which data sets were parametric and normally distributed and which were not. All colony count data was shown not to be normally distributed and nonparametric in nature ($\alpha \leq 0.5$). Data sets from the three trials

were combined and differences between the distributions were determined using the Mann-Whitney U test ($\alpha = 0.5$). Comparisons included the differences between the Control and Treatment microcosms for both the Environmental and Clinical strains of *V. vulnificus* and the differences between the Environmental and Clinical strains in both the Control and Treatment microcosms. Data sets collected from the HCI were also determined to be nonparametric using Shapiro-Wilkes tests. The HCI data was analyzed using the Mann-Whitney U test and compared the differences in relative proportions of 6 major categories, rod-shaped, transition, cocci-shaped, live, dead and unstained cells. These comparisons were run to look at the differences between Clinical and Environmental strains within both the Control and Treatment microcosm, as well as the differences between the Control and Treatment microcosm within a given strain. All p-values were adjusted using the False Discovery Rate adjustment to help reduce the type 1 error rate. All statistical tests were conducted in RStudio Version 1.1.463 (Boston, MA).

3 RESULTS

3.1 Tracking Culturability of *Vibrio vulnificus* in Microcosms at Two Salinities

The culturability of *Vibrio vulnificus* was tracked over a time series and distribution differences were analyzed using the Mann-Whitney U test. Within the Environmental strain, the control population (11 ppt) went from $6.15\text{E}7 \pm 1.07\text{E}7$ CFU/mL on the first day of the experiment to $2.20\text{E}7 \pm 5.00\text{E}6$ CFU/mL on the final day. Conversely, the treatment population, which began with a density of $6.02\text{E}7 \pm 8.55\text{E}6$ CFU/mL, declined to $0.00\text{E}0 \pm 0.00\text{E}0$ CFU/mL by day 8 and remained at the same density on day 9. While the population of *V. vulnificus* in the treatment microcosm did not lose complete culturability until day 8, a major decline in culturable cells can be seen beginning on day 3. The difference between these two populations can be seen in Figure 12 and was significantly different ($p = 2.54\text{E}-3$).

The comparison of the control and treatment populations for the Clinical strain of *V. vulnificus* can be seen in Figure 13. The control population had a starting density of $6.40\text{E}7 \pm 3.78\text{E}6$ CFU/mL on the first day of the trial and had a final density of $8.50\text{E}6 \pm 6.00\text{E}5$ CFU/mL. The treatment population began with a density of $6.34\text{E}7 \pm 1.63\text{E}7$ CFU/mL but declined to $0.00\text{E}0 \pm 0.00\text{E}0$ CFU/mL on day 9. As with the Environmental strain, the Clinical population in the treatment microcosm showed major declines in culturability beginning on day 4, while the full shift to VBNC occurred on day 9. The treatment population was shown to be significantly different from the control ($p = 1.04\text{E}-5$).

Within the control group, the population of the Environmental and Clinical strains responded differently over time. This comparison was marginally significant ($p = 1.36E-2$). However, within the treatment group, the two strains did not respond in a way that was significantly different from one another ($p = 9.02E-1$). These data help to support the first hypothesis (H_1) that *Vibrio vulnificus* will lose culturability in elevated salinity, and the second hypothesis (H_2) that standard cultivation techniques will not be a reliable way to detect *V. vulnificus* outside of its salinity tolerance range (Figure 14). However, this data does not support the third hypothesis (H_3) that the Environmental strain will be more resilient to osmotic stress than the Clinical strain.

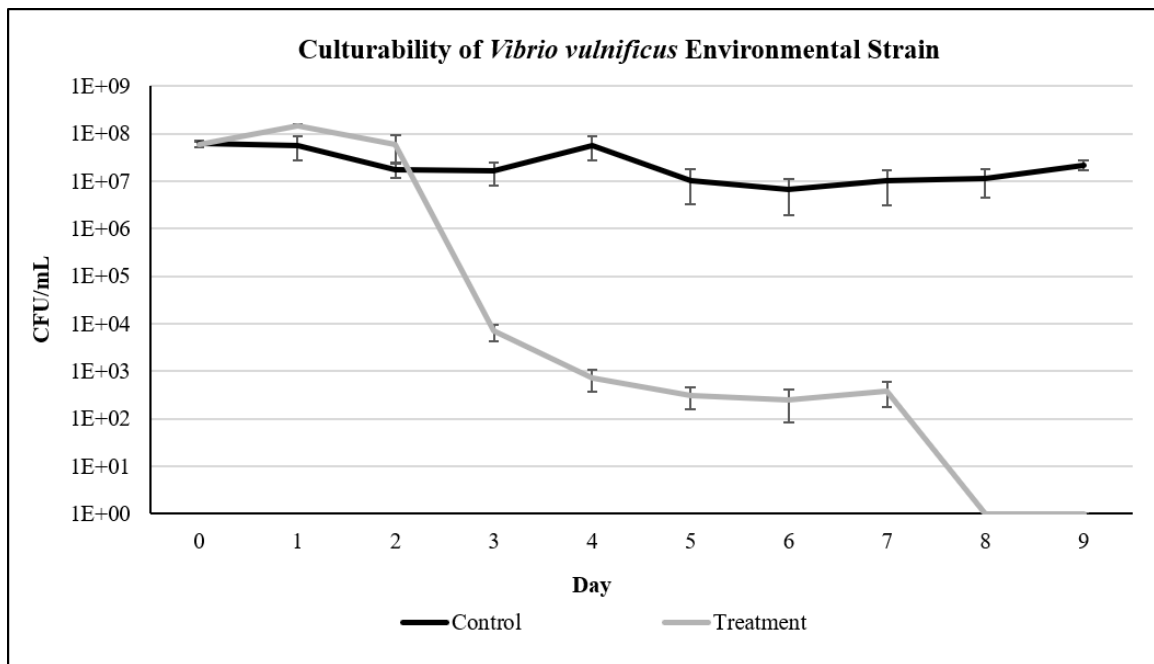


Figure 12 Comparison of culturability over time for *V. vulnificus* Environmental strain (vcgE) in a control (11 ppt) and treatment (35 ppt) microcosm. Graph shows the averages of the duplicate plate counts among the three replicate trials with standard error.

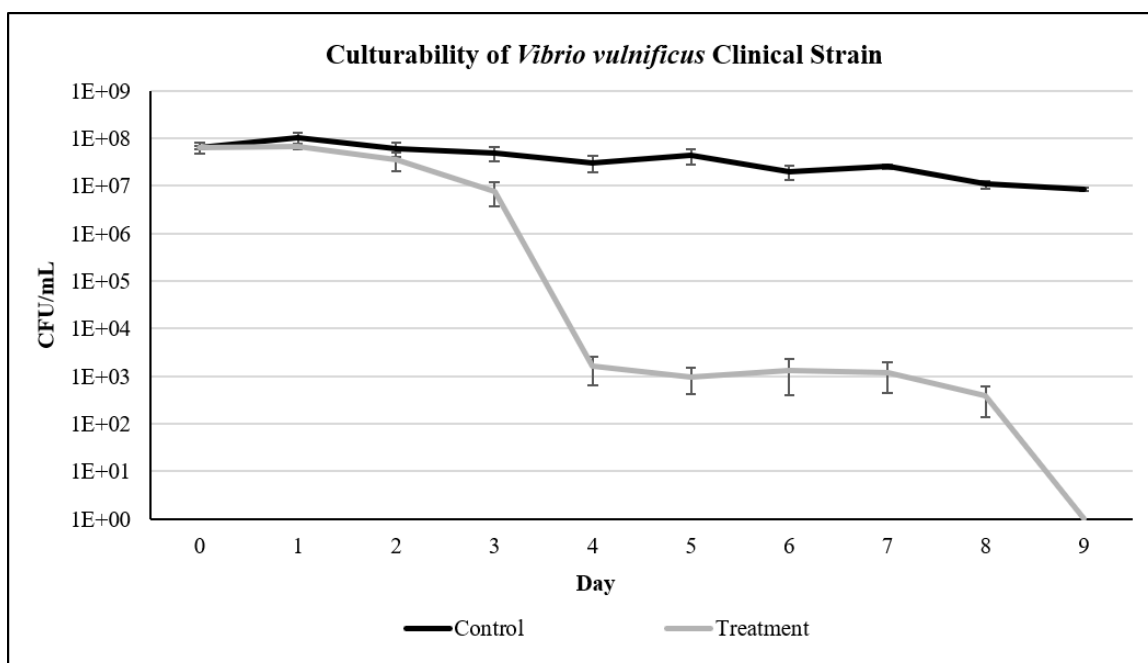


Figure 13 Comparison of culturability over time for *V. vulnificus* Clinical strain (vegC) in a control (11 ppt) and treatment (35 ppt) microcosm. Graph shows the averages of the duplicate plate counts among the three replicate trials with standard error.

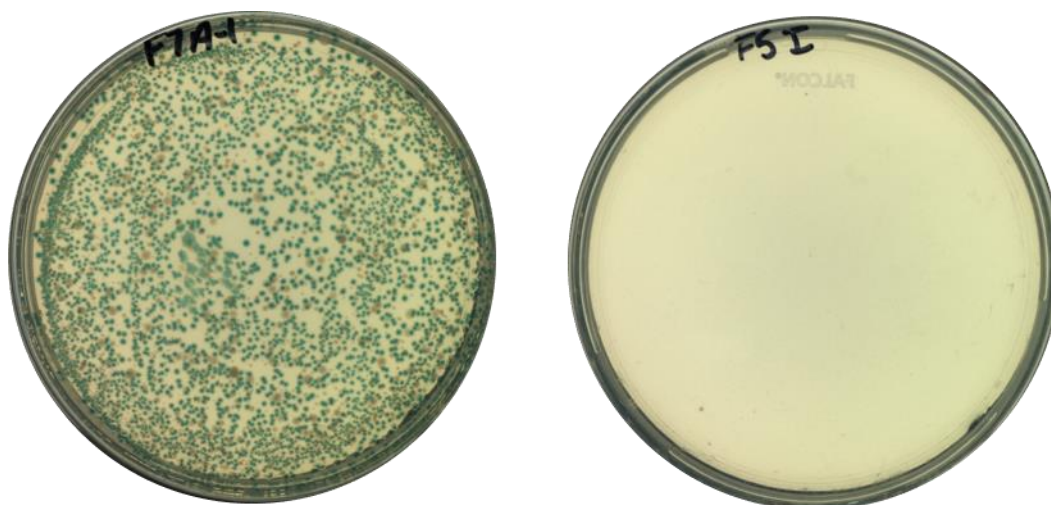


Figure 14 Representative CHROMagar *Vibrio* plates. On the left is a plate illustrating the growth of a control population. The plate on the right shows the complete decline of culturability of *V. vulnificus* after 9 days in the treatment microcosm.

3.2 *BacLight* Live/Dead Viability Assay Using the High Content Imager

The population of live, dead and unstained *V. vulnificus* cells was measured by the *BacLight* Live/Dead Viability Assay and the relative proportions were compared between treatments within the same strain and between the strains within the same treatment using

the Mann-Whitney U test. On the first day on the experiment, the population of Environmental *V. vulnificus* cells within the control microcosm was comprised of 77.88% live cells, 4.47% dead and 17.64% unstained (Figure 15). Conversely, the final day of the experiment yielded a population with 75.12% live cells, 3.99% dead and 20.89% unstained. Figure 15 shows a trend of consistency among the three proportions of cells throughout the experiment. The population within the treatment microcosm began the experiment with 81.61% live cells, 0.51% dead and 17.88% unstained, and ended with 86.99%, 8.85% and 4.16% respectively (Figure 16). Despite the increase in proportion of dead cells at the end of the experiment, the majority of the cells in the treatment microcosm remained alive. This data helps support the first hypothesis (H_1) that elevated salinity will cause *V. vulnificus* to become VBNC. There were, however, significant differences found in the proportion of live, dead and unstained cells between the control and treatment microcosms for the Environmental strain ($p = 1.98E-5$, $p = 5.36E-15$, $p = 1.41E-7$ respectively).

For the Clinical strain, the control population began with 83.91% live cells, 6.08% dead and 10.01% unstained. At the end of the time series the proportions for live, dead and unstained cells were 79.32%, 1.64% and 19.04% respectively (Figure 17). Within the treatment microcosm, the population was initially comprised of 74.76% live cells, 0.38% dead and 24.86% unstained which shifted to 95.36%, 1.74% and 2.91% for each category on the final day of the experiment (Figure 18). Both control and treatment microcosms demonstrated an increase in the proportion of unstained cells in the middle days of the experiment, however both showed decreasing proportions of this population towards the end of the time series. Additionally, the small proportion of dead cells at the end of the

experiment in the treatment microcosm (1.74%) also helps support the first hypothesis (H_1). However, the proportions of the live, dead and unstained cells differed significantly between the control and treatment microcosms for the Clinical strain ($p = 6.60E-16$, $p = 6.60E-16$, $p = 6.60E-16$).

In the control microcosms, there were significant differences in the proportion of live and unstained cells ($p = 6.60E-16$, $p = 6.60E-16$) between the Environmental and Clinical strains but not in the proportion of dead cells ($p = 1.71E-1$). The same is true for the treatment microcosms; the proportion of live and unstained cells differed significantly between the strains ($p = 2.36E-4$, $p = 1.14E-2$) but not in the dead cell proportion ($p = 4.65E-1$). These data do not support the third hypothesis (H_3) that the Environmental strain of *V. vulnificus* will be more resilient to osmotic stress than the Clinical strain (Figures 19 and 20).

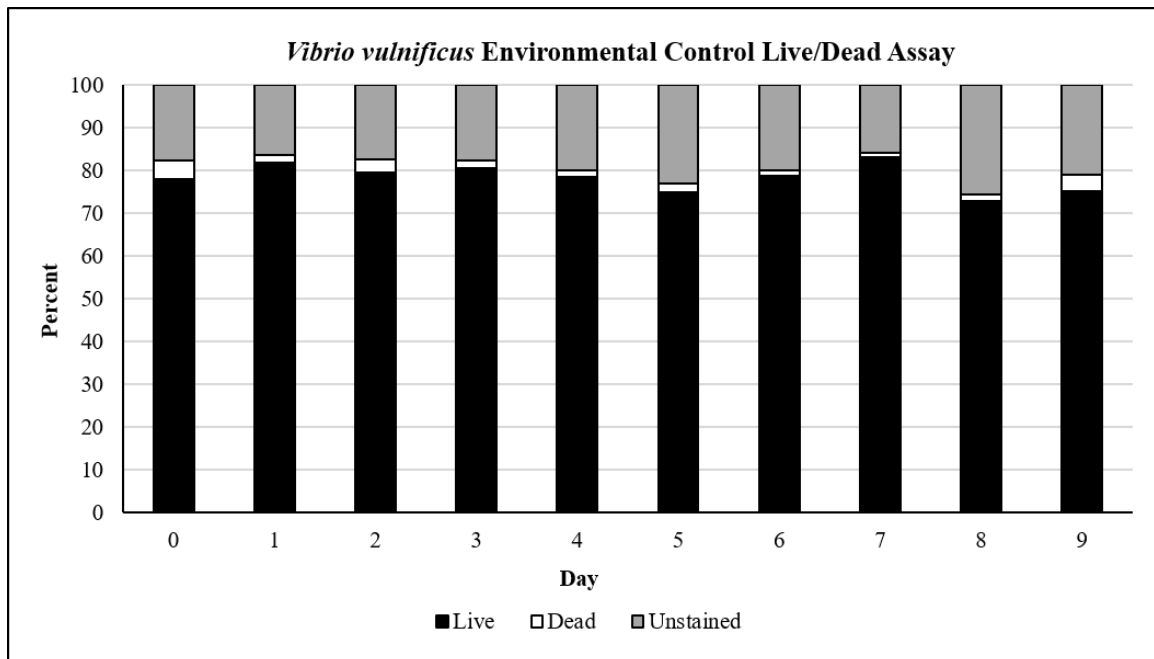


Figure 15 Relative proportions of live, dead and unstained cells over a time series for *Vibrio vulnificus* Environmental strain (vcgE) in the control microcosm (11 ppt).

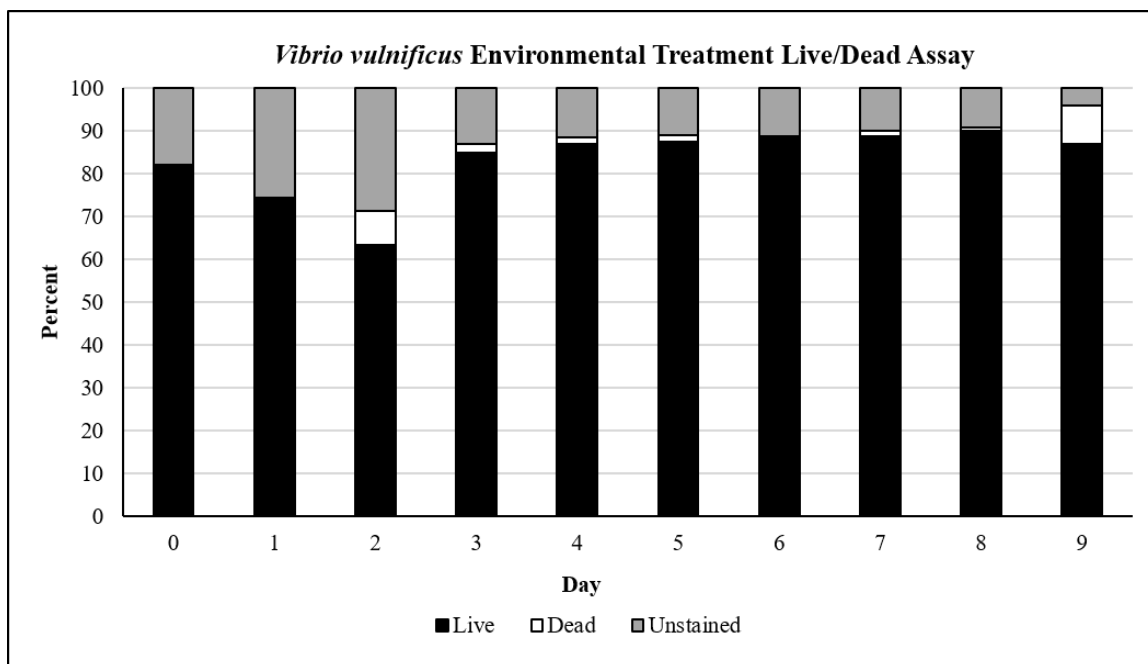


Figure 16 Relative proportions of live, dead and unstained cells over a time series for *Vibrio vulnificus* Environmental strain (vcgE) in the treatment microcosm (35 ppt).

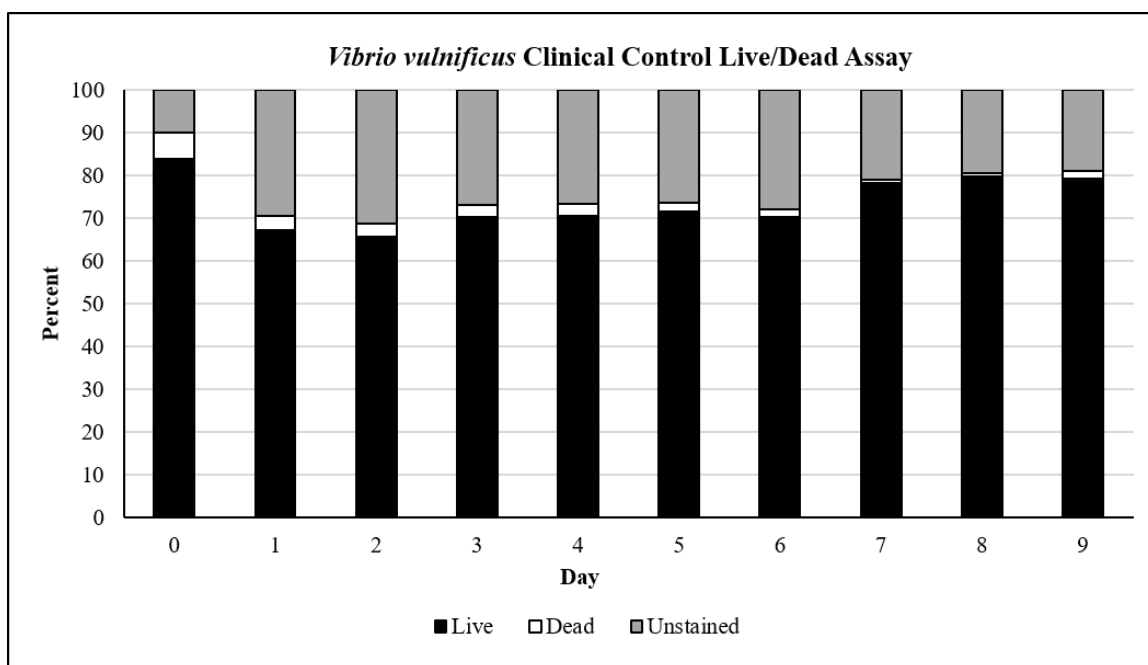


Figure 17 Relative proportions of live, dead and unstained cells over a time series for *Vibrio vulnificus* Clinical strain (vcgC) in the control microcosm (11 ppt).

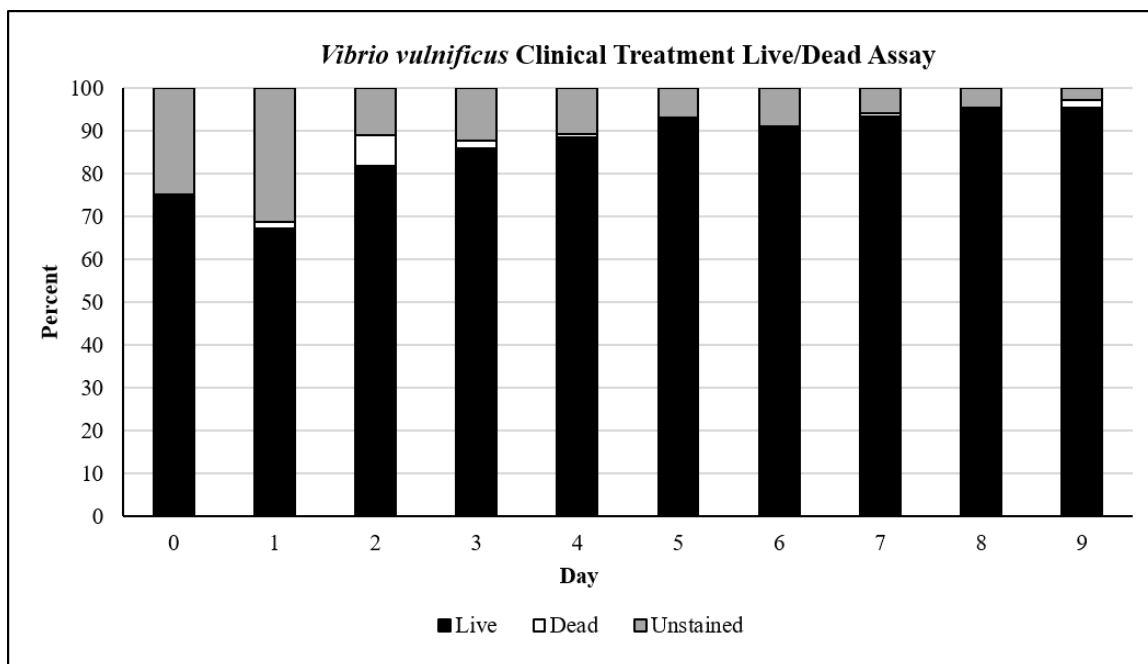


Figure 18 Relative proportions of live, dead and unstained cells over a time series for *Vibrio vulnificus* Clinical strain (vcgC) in the treatment microcosm (35 ppt).

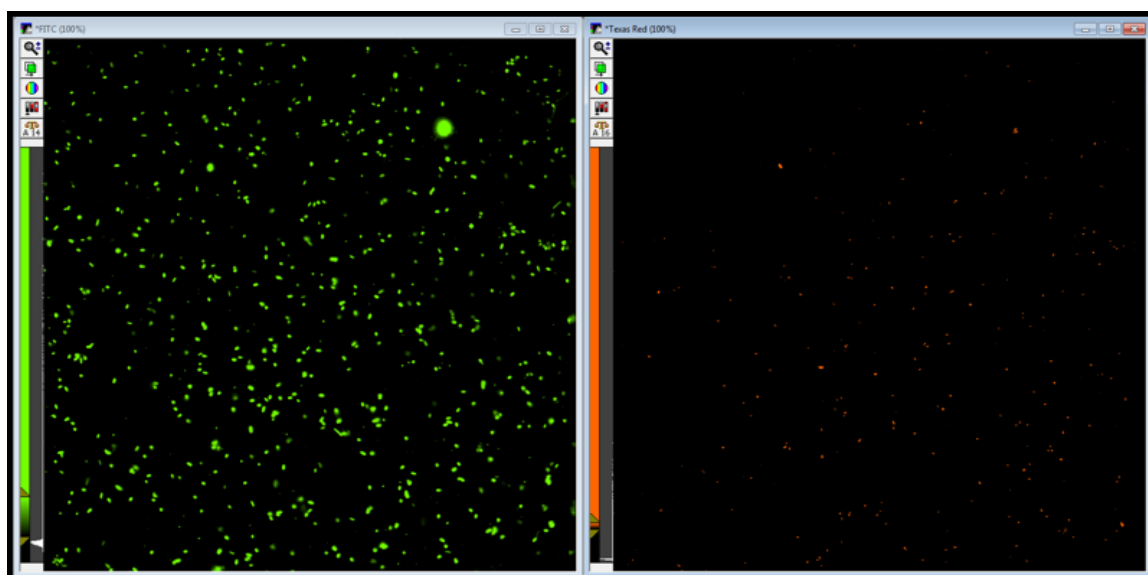


Figure 19 Relative proportion of live *V. vulnificus* cells, shown in the left image, and dead cells, shown in the right image, for a representative control population at the end of the time series.

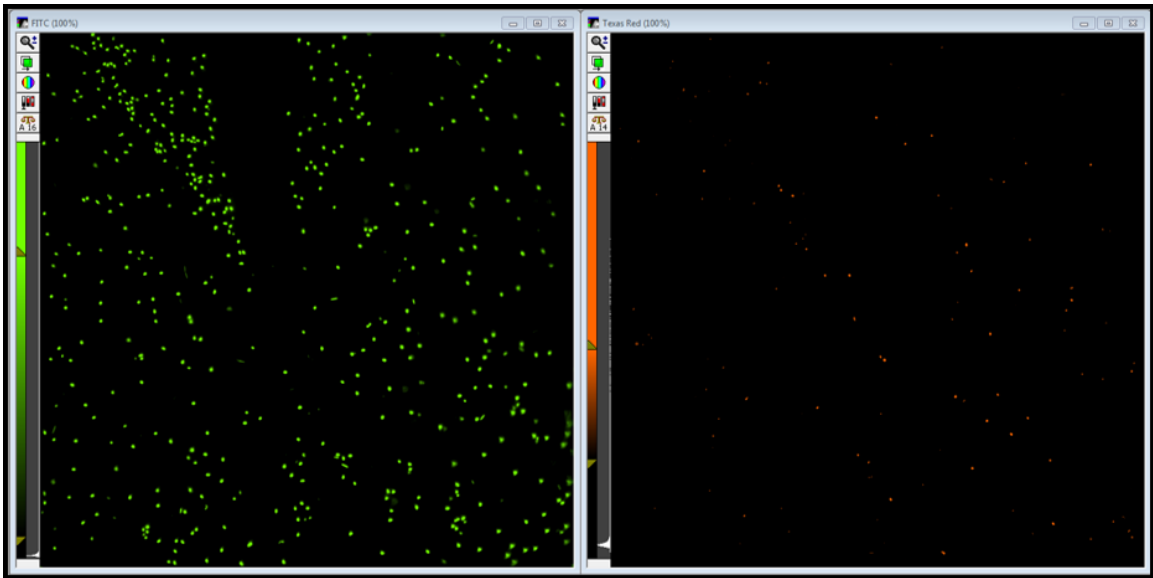


Figure 20 Relative proportion of live *V. vulnificus* cells, shown in the left image, and dead cells, shown in the right image, for a representative treatment population at the end of the time series.

3.3 Morphological Analysis Using the High Content Imager

Samples taken daily from each microcosm were analyzed using the MetaXpress software package (version 5.3.0.5). The cells were counted and divided into 3 major groups, Rods, Cocci and Transition, depending on size and shape constraints. The Environmental strain of *V. vulnificus*, in the control microcosm, had initial population proportions of 71.20% rods, 12.24% cocci and 16.56% transitional cells. At the end of the time series, those populations were 54.30%, 12.04% and 33.66% respectively. Overall, there was a 23.73% decline in the number of rod-shaped cells, a 1.66% decline in the cocci population and 103.26% increase in the proportion of transitional cells. The shift in population proportions can be seen in Figure 21. Conversely, the initial proportions of each cell category within the treatment microcosm for the Environmental strain was 67.80% rods, 13.89% cocci and 18.31% transitional cells. Unlike the control microcosm, the treatment populations were all roughly equivalent on the last day of the experiment, with 31.99% rods, 35.86% cocci and 32.15% transitional cells (Figure 22).

This treatment showed a 52.81% decline in the proportion of rod-shaped cells, a 158.22% increase in cocci and a 75.57% increase in transitional cells. A significant difference was found between the control and treatment microcosms for the Environmental strain in both the populations of rods and cocci ($p = 5.04\text{E-}6$ and $p = 6.60\text{E-}16$) throughout the time series. However, the proportion of transitional cells did not differ between the control and treatment microcosms ($p = 3.02\text{E-}1$).

In the control microcosm of *V. vulnificus* Clinical strain, the initial population proportions were 71.02% rods, 11.20% cocci and 17.79% transitional cells. By the end of the experiment, the population percentages had shifted to 54.67% rods, 16.35% cocci and 28.98% transitional cells (Figure 23) marking a 23.01% decline in rods, 46.03% increase in cocci and 62.91% increase in transitional cells. In the treatment microcosm however, the population proportions went from 70.62% rods, 13.21% cocci and 35.40% transitional cells at the beginning of the experiment to 39.93%, 24.68% and 35.40% respectively at the end (Figure 24). Overall, the proportion of rods decreased by 43.46% in this treatment with increases of 86.75% and 118.92% for the cocci and transitional cells. For the Clinical strain, the populations of rods, cocci and transitional cells differed significantly between control and treatment microcosms ($p = 6.60\text{E-}16$, $p = 6.60\text{E-}16$, $p = 1.34\text{E-}13$ respectively).

Population proportions of the rod-shaped cells ($p = 4.84\text{E-}6$) and transitional cells ($p = 3.60\text{E-}8$) differed significantly between the Clinical and Environmental strains in the control microcosm but not for the cocci ($p = 1.27\text{E-}1$). Conversely, the two strains did not differ in the proportion of rod-shaped cells ($p = 1.71\text{E-}1$) and transitional cells ($p = 7.83\text{E-}1$) in the treatment microcosms but did, however, differ significantly in the

proportion of cocci ($p = 2.33\text{E-}2$). The differences shown in the response of the treatment microcosm compared to the control help provide support to the first hypothesis (H_1) that *Vibrio vulnificus* will become Viable But Nonculturable in response to elevated salinity. However, the greater decline in rod-shaped cells and increase in cocci for the Environmental strain in the treatment microcosm does not yield support for the fourth hypothesis (H_4) that the Environmental strain will be more resilient than the Clinical strain to osmotic stress. Finally, the presence of all three population types (rods, cocci and transitional cells) at the end of both treatment experiments, does not support the third hypothesis (H_3) that *Vibrio vulnificus* will shift completely from 3 μm curved rods to 0.6 μm cocci during the time course of the experiment (Figure 25).

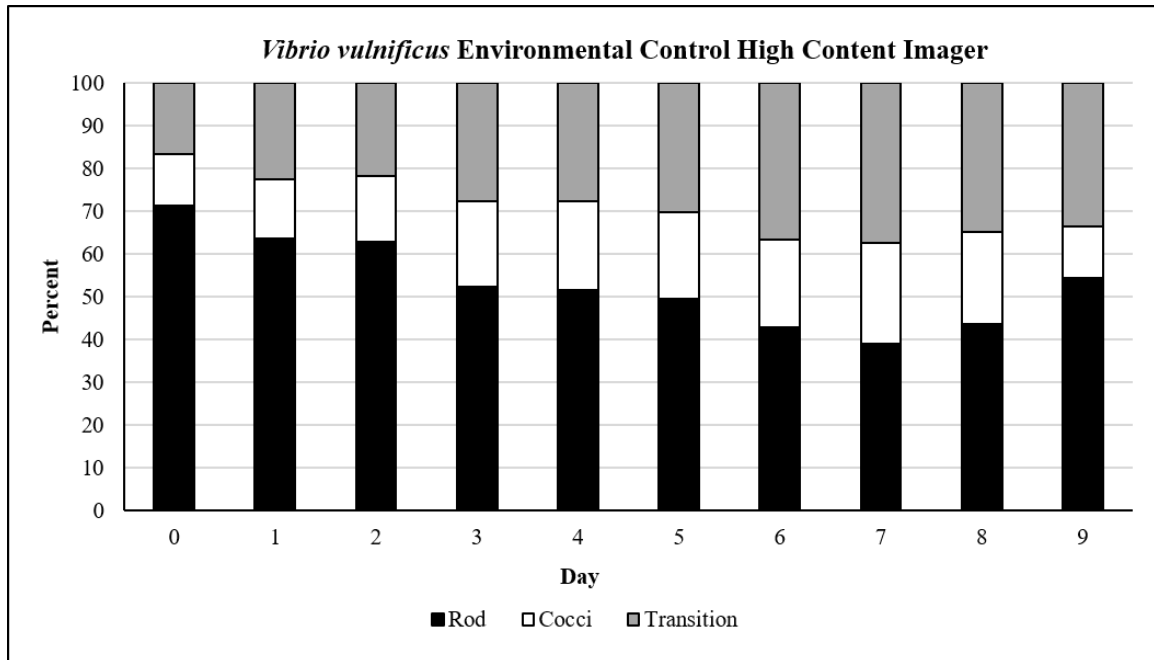


Figure 21 Relative proportions of rods, cocci and transitional cells over a time series for *Vibrio vulnificus* Environmental strain (vcgE) in the control microcosm (11 ppt).

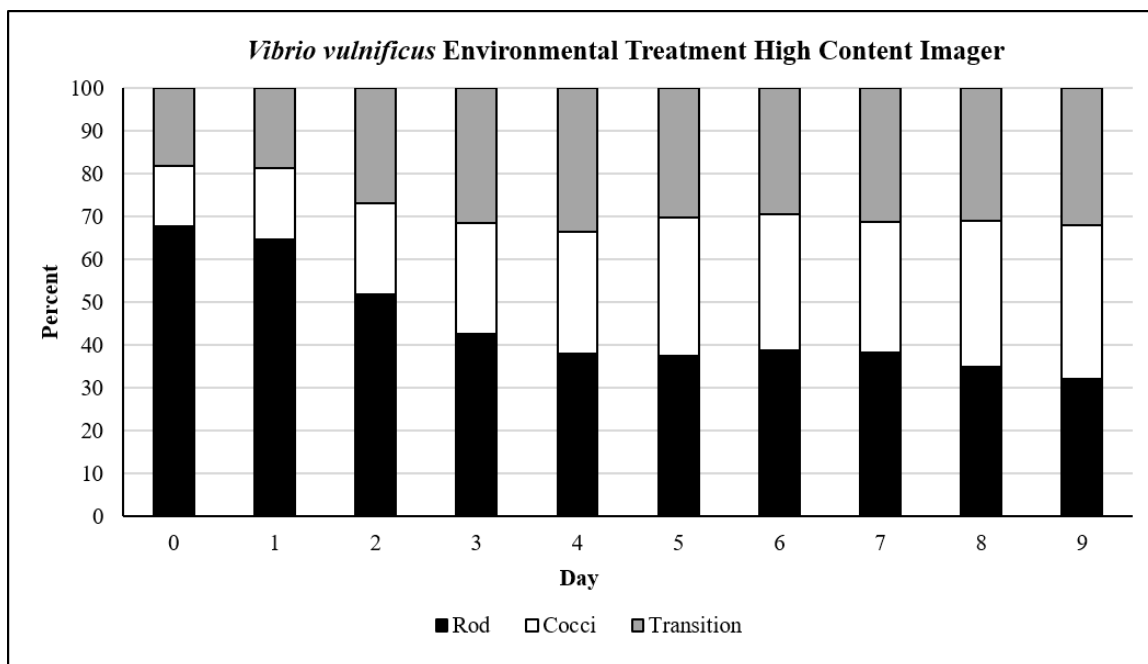


Figure 22 Relative proportions of rods, cocci and transitional cells over a time series for *Vibrio vulnificus* Environmental strain (vcgE) in the treatment microcosm (35 ppt).

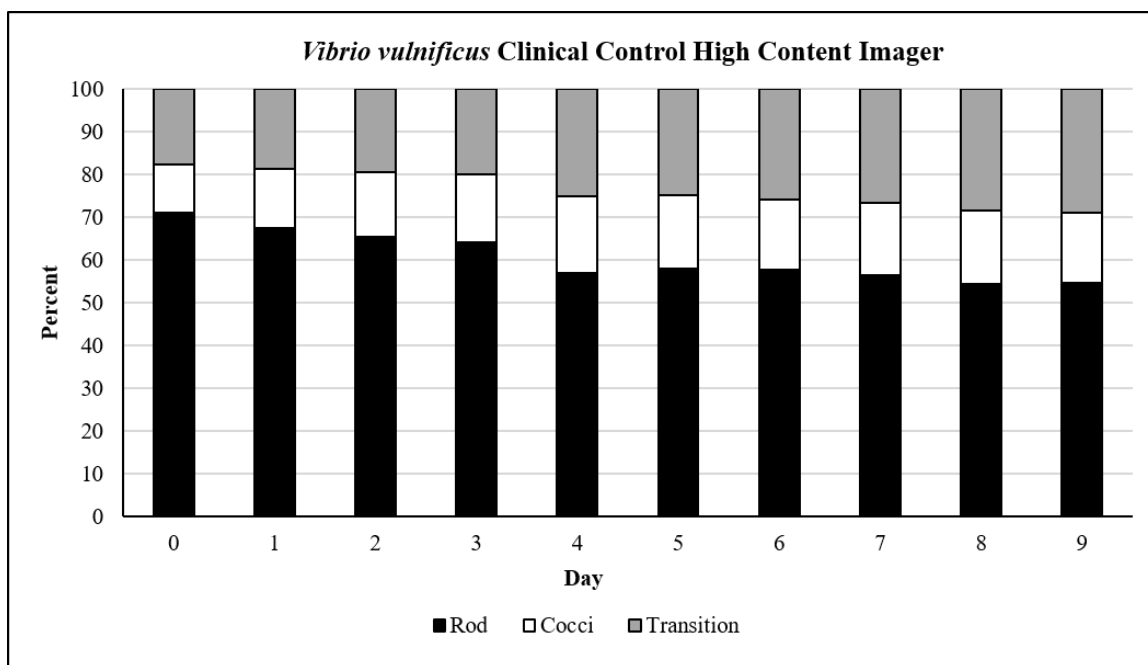


Figure 23 Relative proportions of rods, cocci and transitional cells over a time series for *Vibrio vulnificus* Clinical strain (vcgC) in the control microcosm (11 ppt).

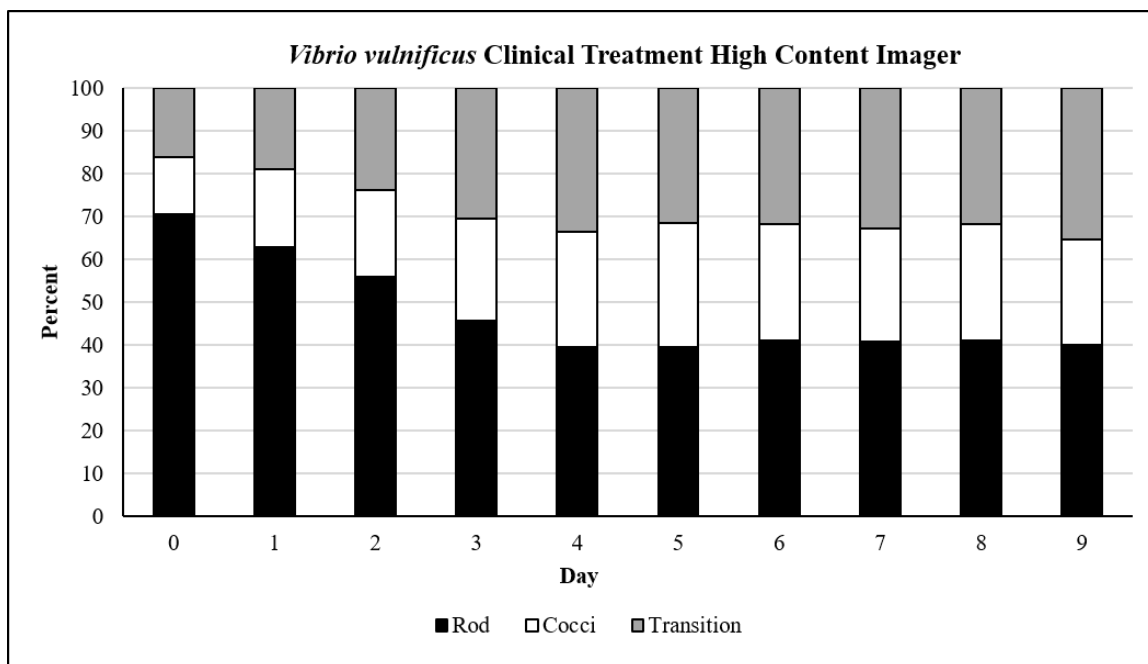


Figure 24 Relative proportions of rods, cocci and transitional cells over a time series for *Vibrio vulnificus* Clinical strain (vcgC) in the treatment microcosm (35 ppt).

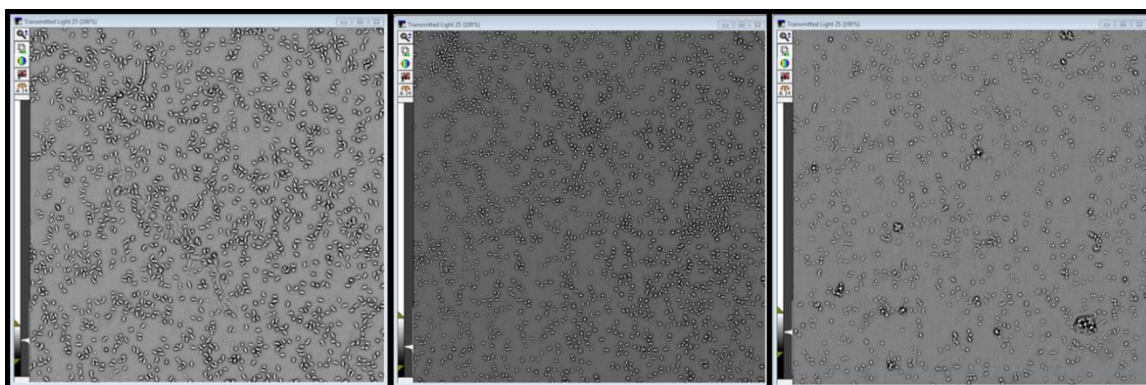


Figure 25 Images showcasing the change in *V. vulnificus* cell shape and size over the course of the time series. The image on the left illustrates a representative population on the day of inoculation. The image in the middle shows the control population at the end of the time series. The image on the right shows the treatment population at the end of the experiment.

4 DISCUSSION

4.1 Methods Development

A major component of this research was to not only understand how the culturability of *Vibrio vulnificus* changed over time when exposed to elevated salinity, but also to determine if those cells remained viable as well as changed their morphology, indicating a true shift into the Viable But Nonculturable state. It was originally proposed to visualize these distinct parameters by utilizing the Biological Devices (BD) Facscanto II Flow Cytometer. This instrument had a Forward Scatter threshold of 1.0 μm and a Side Scatter threshold of 0.5 μm . With a hypothetical VBNC *Vibrio vulnificus* cell being 0.6 μm across, this instrument should have captured the population even at its smallest size. However, despite samples containing cells much larger than the threshold capabilities of the BD Facscanto II, the populations could not be centered in the scatterplot to allow their size to be measured correctly. The flow cytometer was able to detect the SYTO 9 and propidium iodide stains however, without size detection, this technique could not gather all of the data needed for this project.

For this reason, the Molecular Devices Image Xpress Micro XLS High Content Imager was chosen as the best method for obtaining both viability data and cell size and shape. Much optimization occurred before this instrument was able to produce reliable images and data for the experiment. Initial image collection was attempted on a 96-well plastic bottom plate (Nunc # 1653) on 60x magnification. *Vibrio vulnificus* cells were visible and could be enumerated and scored for fluorescence, however, information

regarding the size or shape of the cell was not obtainable at this magnification. With the switch to the 100x magnification came a switch to a 384-well optical plate. Two types were used during optimization: a 384-well plastic bottom plate (Nunc # 142761) and a 384-well glass bottom plate (Nunc # 240074). Ultimately, the glass bottom plate had the least variability in the bottom which led to the least distortion of the images.

Furthermore, optimization of the imaging software had to be done in order to take consistently reliable photos of the samples across the time series and replicates. The imaging software typically utilizes an auto-focus mechanism to find the bottom of the plate and then focus on the cells. However, this program only runs on magnifications lower than 100x due to the larger working distance of the objective. To compensate for the lack of auto-focusing abilities, a specialized journal was written to help automate the imaging process. To run the 100x objective on a program, the manual focus distance of the cells was determined and entered into the journal. While each plate differed, the distance needed to focus of the cells ranged from approximately 10,000 to 13,000 μm above the objective stage.

Next, offset distances and well-to-well variability were calculated for the journal. Offset distances told the machine how different the focus was between the primary wavelength, in this experiment it was Transmitted Light 25, and the other wavelengths, FITC and Texas Red, to be imaged. On average, the focus of the Transmitted Light 25 images was 0.7 μm lower than the focus of the two fluorescent wavelengths.

Additionally, the well-to-well variability was calculated to tell the machine how much higher or lower to move the objective when switching to the next well, preventing the objective from contacting the bottom of the plate and risking damage or coming out of

the immersion oil and creating bubbles. Across the three 384-well plates used, the average variability between wells was 5 to 10 μm .

Lastly, to ensure the best quality of the images, especially for the size and shape analysis in the Transmitted Light 25 pictures, acquisition and post-processing functions were added into the journal. A Z-stack of 8 images was included during acquisition to take 8 individual images, spaced 0.1 μm apart, which were then combined. This allowed for the best focus of as many cells as possible to be combined and visualized. After the creation of the Z-stack image, a background smoothing program was employed to remove any debris or shadows that were determined to not be true cells by the program.

Sample collection and preparation for screening also had to be optimized. Initially, formaldehyde, diluted to a final concentration of 4% was used to fix the cells after staining with the *BacLight* Live/Dead Viability Assay. With this fixative, issues were encountered with the *V. vulnificus* cells not retaining the dye. After consultation with ThermoScientific, glutaraldehyde, diluted to a final concentration of 4% was chosen as the most appropriate fixative for retaining the viability dye. Additionally, samples were to be stained and fixed for each day of the experiment until the treatment population lost culturability, at which point the samples would be plated into the Nunc 384-well glass bottom optical plate (part # 240074) for imaging. During a preliminary experiment, it was determined that cells were clumping excessively while being stored at 4 °C, which made enumeration and distinction difficult. To combat this, samples were stained, fixed, plated and centrifuged daily in the 384-well plate to prevent cell clumping.

Once the images were collected for all samples and all replicates, analysis for fluorescence and size could be optimized. The software's pre-installed "multi-wavelength

analysis” was used to determine cell viability, however, certain thresholds of size and intensity were set. While the size threshold of 0.5 to 2.5 μm wide remained consistent throughout the multi-wavelength analysis, the intensity thresholds varied based on cell density, clumping and overall uptake of the stains. These values were determined based on the individual set of samples being run but were approximately 450 for Transmitted Light 25, 150 for FITC and 150 for Texas Red.

The final aspect of the methods development and optimization was the creation of a novel custom analysis module on the MetaXpress Software (version 5.3.0.5). This analysis contained several pre-scoring filters to help smooth the background of the images as well as the edges of the cells to obtain more accurate measures of cell length. Cell length was chosen because it measures the longest distance across any object defined as a cell. This would eliminate the orientation of a cell as a factor in determining its true size. An intensity threshold of 1000 on average, helped to distinguish smaller cells from bright spots in the image. A total of three categories were used to define a cell’s shape; rods, cocci and transitional cells. Since this software measures a cell by counting the pixels that pass the intensity threshold, the distances, in μm , were not as well defined as in the literature. To determine the most practical length, thresholds for each of the groups, cells that were considered to be true rods, mostly from day 0 of the experiment, and cells that were considered to be cocci, mostly from day 9, were individually measured. The values from these individual cell measurements were used to categorize rods (1.6 to 2.5 μm) and cocci (0.5 to 1.1 μm). Those cells that fell in between the thresholds for the two groups became the transitional cells.

4.2 Culturability of *Vibrio vulnificus* in Two Salinity Microcosms

Results from the culturability study helped to support the first hypothesis (H_1) that *Vibrio vulnificus* would become Viable But Nonculturable when exposed to elevated salinity (35 ppt). This was demonstrated equally well in both the Clinical (*vcgC*) and Environmental (*vcgE*) strains (Figures 12 and 13). In both cases, population densities began on the order of 10^7 CFU/mL and declined to 10^0 CFU/mL by day 8 and 9. These data agree with the trends found in a study investigating the effects of decreased temperature (5 °C) on the induction of the VBNC state in *V. vulnificus* (Oliver 1996). Compared to this study, the loss of culturability due to elevated salinity (35 ppt) came about 4 days after what was reported for temperature, indicating that salinity may not be as stressful to this bacterium as temperature. The results from this study also agree with those found in the first ever systemic study of pathogenic *Vibrio* species in the Indian River Lagoon (Barbarite 2016). It was shown in this study that *V. vulnificus* exhibited a strong negative correlation with salinity, having an optimal range between 5 and 25 ppt. It was also shown that *V. vulnificus* was never cultivated from sediment at the beach (35 ppt) or from fish found in waters where the salinity was over 33 ppt. The lack of this pathogen at such elevated salinities may be explained by it becoming VBNC and no longer being culturable.

This lack of culturability for *V. vulnificus* at salinities above its tolerance range, may indicate that standard culturing techniques using routine bacteriological media are not effective in determining the presence of this pathogen in certain areas. Since this bacterium is not tested for or included in any state water quality monitoring, only research projects can provide information about the abundance and distribution of *V.*

vulnificus in the environment (Yamazaki and Esiobu 2012). However, many microbiological research projects looking for *V. vulnificus* in the environment rely on bacteriological media, such as CHROMagar *Vibrio*, TCBS and mCPC. These methods may prove very useful within the salinity tolerance range of *V. vulnificus*, but above that range, it may not be as practical.

This inability to detect *V. vulnificus* in certain environments is important because this species has been shown to retain its virulence upon entering the VBNC state (Oliver and Bockian 1995). This makes the accurate detection of this pathogen outside of its tolerance range critical to human safety. It is likely that molecular techniques, such as real time PCR, may be more reliable in detecting VBNC *V. vulnificus* cells in the environment than standard culturing techniques. For these reasons, the data shown in this experiment help to support the second hypothesis (H₂) that standard bacteriological media may not be an appropriate technique to detect *V. vulnificus* above its salinity tolerance range.

It was also shown that, between strains in the control group, there was a marginal difference in the response of *V. vulnificus* during the time series. This was likely due to a degree of variability expressed in the control population replicates in the Environmental strain (Figure 12). There were some instances where the population densities declined slightly during the time series that did not occur in the Clinical strain (Figure 13). Despite the strains both remaining within the same order of magnitude throughout the experiment, the day-to-day variation within the Environmental strain was enough for a statistical test to indicate a difference. However, in the treatment microcosms, there was no statistical difference indicated between the two strains. This means that the third (H₃)

hypothesis that the Environmental strain would be more resilient to osmotic stress than the Clinical strain was not supported by the data. Both populations were shown to decrease in approximately the same fashion over time and across the replicates. Despite the fact that there were no statistical differences in how the two strains reacted in response to the treatment, the data does indicate an interesting trend of the Environmental strain not only beginning its decline in culturability before the Clinical strain, day 3 instead of day 4, but also losing culturability first, on day 8 instead of day 9. This further provides some evidence against the third hypothesis (H₃).

4.3 *BacLight* Live/Dead Viability Assay Using the High Content Imager

Techniques that utilize cell-permeable and cell-impermeable dye combos, such as the *BacLight* Live/Dead Viability Assay, can be useful tools for determining if a population of *Vibrio vulnificus* that has lost culturability is indeed still viable, indicating entry into the Viable But Nonculturable state (Oliver 2009). Across all of the replicates, for both strains and both control and treatment microcosms, the proportion of dead cells never exceeded 10% on any given day. In fact, the percentage of dead cells within a given population was most often around the 2-3% mark. This overwhelming lack of dead cells provides evidence to the first hypothesis (H₁) that *V. vulnificus* is becoming VBNC as a response to elevated salinity (35 ppt) as opposed to dying due to osmotic stress. An additional trend regarding the population of live cells is shown with proportions regularly above 70% but in some cases as high as 95% of all cells in the sample being recorded as alive. This trend is particularly true in the case of the Clinical strain in the treatment microcosm, where the population of cells at the end of the experiment, when no

culturable cells were recovered, had proportions of 95.36% live, 1.74% dead and 2.91% unstained (Figure 18).

Not only did the Clinical strain show such a small proportion of dead cells at the end of the experiment, it had far less than the Environmental strain (Figure 16) exposed to the same treatment (8.85%). Although there were no significant differences in population of dead cells between the strains in the treatment microcosm, the Clinical strain actually responded more favorably than the Environmental strain. This does not support the third hypothesis (H₃) that the Environmental strain would be more resilient to osmotic stress than the Clinical strain. This trend is similar to what was seen in the Oliver et al (1995) study which induced the VBNC state in both strains of *V. vulnificus* using water temperature of 5 °C. This study also showed remarkably similar trends between the two strains, and therefore did not show a difference in resilience between strains.

These data also bring up an intriguing trend that shows a moderate proportion of cells in some cases not taking up either of the two DNA binding dyes. Across all trials, there was approximately 20% of the population of cells being scored as unstained. No strain or treatment appeared to be correlated with this trend but previous research using a similar stain coupled with direct viable counts noted some discrepancies between the cells counted viable using the stain and those counted using DVC (Oliver et al 1995).

4.4 Morphological Analysis Using the High Content Imager

Utilization of the Molecular Devices Image Xpress Micro XLS High Content Imager was not only novel for the instrument, but also for the detection of a morphological shift of *Vibrio vulnificus* as it becomes Viable But Nonculturable. This technique helped to provide unique information regarding the physical changes of *V.*

vulnificus, both Clinical and Environmental strains, in both a control (11 ppt) and treatment (35 ppt) microcosm. Several interesting trends appeared after analyzing the data. Most notably, all populations across both strains and treatments showed changes in the relative proportion of rods, cocci and transitional cells. This was not an expected result, as the control population did not lose its culturability throughout the entirety of the experiment. However, the Environmental strain had decreases in the proportion of rods and cocci of 23.73% and 1.66% respectively, while having a large increase (103.26%) in transitional cells (Figure 21). While the Clinical strain saw a similar decrease (23.01%) in the rod-shaped cells, it had increases in the cocci and transitional cells of 46.03% and 62.91% (Figure 23). It is likely that in the case of the control populations, including both Environmental and Clinical strains, that the cells became nutrient deprived over time and began to shrink. As a result, these smaller cells would begin to fall into the categories of transitional cells and cocci, thus shifting the proportions.

Equally as intriguing, is the fact that in the treatment populations, there was not a full conversion from rod-shaped cells to cocci. This is true for both the Clinical and Environmental strains, which never showed proportions of cocci above 40%. Not only does this fail to support the fourth hypothesis (H₄) that VBNC *V. vulnificus* cells would undergo a complete shift in morphology, but it also indicates that much more is occurring during this process than just a change in cell size and shape. This is made even more obvious by the changes in cell morphology within the control populations. What this means is that a simple decrease in cell size within a *V. vulnificus* population may not actually indicate a shift to becoming VBNC. Conversely, a true transition into the VBNC state for this pathogen may not be concurrent with a complete population shift from 3 μ m

curved rods to 0.6 μm cocci. As these cells are losing culturability, many changes, such as decreased DNA and RNA synthesis, decreasing metabolic function as well as changes in cell membrane composition, are occurring (Oliver 2009).

Another interesting trend within the treatment populations is that the two strains did not respond in the same fashion. The Environmental strain had a decrease in rod-shaped cell proportions of 52.81% and an increase in cocci proportions of 158.23% while the Clinical strain had a decrease in rods of only 43.46% and an increase of 86.75% in the proportion of cocci. This indicates that the third hypothesis (H_3), stating that the Environmental strain would be more resilient to osmotic stress, is not supported. Collectively, however, both strains within the treatment group showed significant differences in population proportions from their control (11 ppt) counterparts.

5 CONCLUSIONS

This study was one of the first to investigate the effects of elevated salinity (35 ppt) on *Vibrio vulnificus* and its ability to enter the Viable But Nonculturable state. Much like this pathogen's other major environmental driver, temperature, *V. vulnificus* responded as initially believed by losing culturability under osmotic stress. This response did not differ between the Clinical (*vcgC*) and Environmental (*vcgE*) strains in common with previous research on this species in cold temperatures (Oliver et al 1995). It was shown in this study that *V. vulnificus* begins to see major declines in culturability around 3 d after inoculation at approximately 10^7 CFU/mL, and complete loss of culturability by 8 d.

Through the use of the *BacLight* Live/Dead Viability Assay, it was determined that the majority of the *V. vulnificus* population (>85%) was alive at the end of the treatment experiments and less than 10% scored as dead, thus these pathogens were not dying in response to the elevated salinity (35 ppt). This information is critically important in interpreting results from the first ever systemic study of pathogenic *Vibrio* species in the Indian River Lagoon (Barbarite 2016). This study indicated that *V. vulnificus* was never recovered from sediments above 35 ppt or fish caught in waters above 33 ppt. It is likely that these bacteria were VBNC and were unable to be cultured. Moving forward, new techniques may need to be employed to better detect this pathogen in recreational waters where the salinity is above the typical tolerance range of this species.

This project was also one of the first to utilize High Content Imaging as a means to count individual bacterial cells as well as measure and record length of each cell. This novel method helped to better understand some of the morphological changes occurring as these bacteria were exposed to both the control and treatment salinities. An intriguing trend was discovered in the control populations which showed decreases in the proportions of rod-shaped cells, and increases in the percentage of cocci and transitional cells. This was, to a lesser extent, the trend that was observed in both strains when exposed to the treatment (35 ppt) salinity. The treatment populations did not see as dramatic a change in population structure as initially expected. It is likely that more processes are going on at a molecular level controlling the shift of *V. vulnificus* into the VBNC state than are represented in their morphologies (Oliver 2009). Despite the uniqueness of this method, and the precise cell measurement information that was able to be collected, it is not recommended that this technique be used as a means of routinely monitoring for VBNC *V. vulnificus* populations. This method, while very useful in a controlled laboratory experiment, was initially very challenging and required much optimization before even a crude analysis could be performed. With further work, this method could become more regularly used in laboratory experiments for screening known populations for viability as well as morphological metrics. For detection of VBNC *V. vulnificus* cells in the environment, particularly above their salinity tolerance range, molecular techniques, such as shotgun sequencing or targeted real time PCR, would be of more use.

Overall, this study has major implications for human health. As shown by Oliver and Bockian (1995), VBNC *V. vulnificus* cells can retain their virulence for some time

and are still capable of causing infection. These cells were also shown to resuscitate and regain all normal cell function in vivo when conditions were more favorable (Oliver and Bockian 1995). Whether or not this process would occur in the same way under osmotic stress is still unknown. However, precautions should still be taken when recreating with an open wound, even when the salinity is above the tolerance range of *V. vulnificus*.

REFERENCES

- Barbarite, G. M. (2016) The Occurrence of *Vibrio vulnificus*, *V. parahaemolyticus* and *V. cholerae* in the Indian River Lagoon, Florida, with implications for human health (Doctoral Dissertation Florida Atlantic University)
- Berney, M., Hammes, F., Bosshard, F., Weilenmann, H., Egli, T., Assessment and Interpretation of Bacterial Viability by Using the LIVE/DEAD BacLight Kit in Combination with Flow Cytometry. *Applied and Environmental Microbiology*, vol. 73, no. 10, 2007, pp. 3283–3290., doi:10.1128/aem.02750-06.
- Blackwell, K. D., & J. D. Oliver (2008). The ecology of *Vibrio vulnificus*, *Vibrio cholerae*, and *Vibrio parahaemolyticus* in North Carolina estuaries. *The Journal of Microbiology* 46.2: 146-153.
- Buck, J. D. (1990). Potentially pathogenic marine *Vibrio* species in seawater and marine animals in the Sarasota, Florida, area. *Journal of Coastal Research*, 6,943-948.
- Center for Disease Control, CDC (2013). National Enteric Disease Surveillance: COVIS Annual Summary, 2011. Atlanta, Georgia: US Department of Health and Human Services, CDC; Available at <http://www.cdc.gov/ncezid/dfwed/pdfs/covis-annual-report-2011-508c.pdf>.
- Center for Disease Control, CDC (2015). National Enteric Disease Surveillance: COVIS Annual Summary, 2013. Atlanta, Georgia: US Department of Health and Human Services, CDC; Available at <http://www.cdc.gov/ncezid/dfwed/pdfs/covis-annual-report-2013-508c.pdf>.

- Daniels, N. A. (2011). *Vibrio vulnificus* oysters: pearls and perils. *Clinical Infectious Diseases*, 52, 788-792.
- Drake, S. L., DePaola, A., & Jaykus, L. A. (2007). An overview of *Vibrio vulnificus* and *Vibrio parahaemolyticus*. *Comprehensive Reviews in Food Science and Food Safety*, 6, 120-144.
- Farmer III, J. J., & Hickman-Brenner, F. W. (2006). The genera *Vibrio* and *Photobacterium*. In *The Prokaryotes* (pp. 508-563). Springer New York.
- FAU Harbor Branch Indian River Lagoon Observatory. *LOBO: Land Ocean Biogeochemical Observatory*, fau.loboviz.com/.
- Florida Department of Health, Bureau of Epidemiology, Division of Public Health Statistics & Performance Management. www.FloridaCHARTS.com
<<http://www.floridacharts.com/charts/OtherIndicators/NonVitalIndNoGrpDataViewer.aspx?cid=0223>>. Accessed February 20, 2019.
- Froelich, B. A., Williams, T. C., Noble, R. T., & Oliver, J. D. (2012). Apparent loss of *Vibrio vulnificus* from North Carolina oysters coincides with a drought-induced increase in salinity. *Applied and Environmental Microbiology*, 78, 3885-3889.
- Gilmore, G., Donohoe, D., Cook, D. & D. Herrema (1981). Fishes of the Indian River Lagoon and adjacent waters, Florida. Tech. Rep. No. 4. Harbor Branch Foundation, Ft. Pierce, FL.
- Griffitt, K. J., & Grimes, D. J., Abundance and distribution of *Vibrio cholerae*, *V. parahaemolyticus*, and *V. vulnificus* following a major freshwater intrusion into the Mississippi Sound. *Microbial Ecology* 65.3 (2013): 578-583.

- Han, F., Pu, S., Hou, A., & Ge, B. (2009). Characterization of clinical and environmental types of *Vibrio vulnificus* isolates from Louisiana oysters. *Foodborne Pathogens and Disease*, 6, 1251-1258.
- Harwood, V. J., Gandhi, J. P., & Wright, A. C. (2004). Methods for isolation and confirmation of *Vibrio vulnificus* from oysters and environmental sources: a review. *Journal of Microbiological Methods*, 59, 301-316.
- Thermofisher LIVE/DEAD BacLight Bacterial Viability and Counting Kit, for Flow Cytometry, www.thermofisher.com/order/catalog/product/L34856.
- Hlady, W. G., & Klontz, K. C. (1996). The epidemiology of *Vibrio* infections in Florida, 1981–1993. *Journal of Infectious Diseases*, 173, 1176-1183
- Jacobs, J. M., Rhodes, M., Brown, C. W., Hood, R. R., Leight, A., Long, W., & Wood, R. (2010). Predicting the distribution of *Vibrio vulnificus* in Chesapeake Bay.
- Johnson, C. N., Bowers, J. C., Griffitt, K. J., Molina, V., Clostio, R. W., Pei, S., ... & Colwell, R. R. (2012). Ecology of *Vibrio parahaemolyticus* and *Vibrio vulnificus* in the coastal and estuarine waters of Louisiana, Maryland, Mississippi, and Washington (United States). *Applied and Environmental Microbiology*, 78, 7249-7257.
- Kildow, J. T. (2008). Phase II, facts and figures, Florida's ocean and coastal economies Report. National Ocean Economic Program, Publication 14.
- Lapointe, B. E., Herren, L. W., Debortoli, D. D., & Vogel, M. A. (2015). Evidence of sewage-driven eutrophication and harmful algal blooms in Florida's Indian River Lagoon. *Harmful Algae*, 43, 82-102.
- Martin, J. B., Cable, J. E., Jaeger, J., Hartl, K., & Smith, C. G. (2006). Thermal and chemical evidence for rapid water exchange across the sediment-water interface by

- bioirrigation in the Indian River Lagoon, Florida. *Limnology and Oceanography*, 51, 1332-1341.
- Motes, M. L., DePaola, A., Cook, D. W., Veazey, J. E., Hunsucker, J. C., Garthright, W. E., ... & Chirtel, S. J. (1998). Influence of Water Temperature and Salinity on *Vibrio vulnificus* in Northern Gulf and Atlantic Coast Oysters (*Crassostrea virginica*). *Applied and Environmental Microbiology*, 64, 1459-1465.
- Newton, A., Kendall, M., Vugia, D. J., Henao, O. L., & Mahon, B. E. (2012). Increasing rates of vibriosis in the United States, 1996–2010: review of surveillance data from 2 systems. *Clinical Infectious Diseases*, 54, S391-S395.
- Nilsson, W. B., Paranjypte, R. N., DePaola, A., & Strom, M. S. (2003). Sequence polymorphism of the 16S rRNA gene of *Vibrio vulnificus* is a possible indicator of strain virulence. *Journal of Clinical Microbiology*, 41, 442-446.
- Nowakowska, J., & Oliver J. D., Resistance to Environmental Stresses by *Vibrio vulnificus* in the Viable but Nonculturable State. *OUP Academic*, Oxford University Press, 1 Apr. 2013, academic.oup.com/femsec/article/84/1/213/588859.
- Oliver, J. D. (2015). The biology of *Vibrio vulnificus*. *Microbiology Spectrum*, 3, 1-10.
- Oliver, J. D., The Viable but Non-culturable State in the Human Pathogen *Vibrio vulnificus*. *FEMS Microbiology Letters* 133.3 (1995): 203-08. Web. 22 July 2017.
- Oliver, J. D., & Bockian, R., In Vivo Resuscitation, and Virulence towards Mice, of Viable but Nonculturable Cells of *Vibrio vulnificus*. *Applied and Environmental Microbiology* 61.7 (1995): 2620-623. Web. 22 July 2017.

- Oliver, J. D., Hite, F., McDougald, D., Andon, N. L., and Simpson, L. M., Entry Into, and Resuscitation From, the Viable but Nonculturable State by *Vibrio vulnificus* in an Estuarine Environment. *Applied and Environmental Microbiology* 61.7 (1995): 2624-630. Web. 22 July 2017.
- Oliver, J. D. Recent Findings on the Viable but Nonculturable State in Pathogenic Bacteria. *FEMS Microbiology Reviews* 34.4 (2010): 415-25. Web. 22 July 2017.
- Oliver, J. D. The Viable but Nonculturable State in Bacteria. *The Journal of Microbiology* 43.S (2005): 93-100. Web. 22 July 2017.
- Oliver, J. D., Warner, R. A., & Cleland, D. R. (1982). Distribution and ecology of *Vibrio vulnificus* and other lactose-fermenting marine Vibrios in coastal waters of the southeastern United States. *Applied and Environmental Microbiology*, 44, 1404-1414.
- Regional Planning Council, East Central Florida. Indian River Lagoon Economic Valuation Update. Love Our Lagoon, Florida Department of Economic Opportunity, 2016, loveourlagoon.com/IRL-Economic-Valuation-Update-07252016.pdf.
- Shaw, K. S., Sapkota, A. R., Jacobs, J. M., He, X., & Crump, B. C. (2015). Recreational swimmers' exposure to *Vibrio vulnificus* and *Vibrio parahaemolyticus* in the Chesapeake Bay, Maryland, USA. *Environment International*, 74, 99-105.
- Smith, N. P. Tidal and Nontidal Flushing of Florida's Indian River Lagoon. *Estuaries* 16.4 (1993): 739. Web. 22 July 2017.
- St. Johns River Water Management District. 2007. The Indian River Lagoon: A National Treasure. <http://www.sjrwmd.com/itsyourlagoon/pdfs>.

- Takemura, A. F., Chien, D. M., & Polz, M. F. (2014). Associations and dynamics of Vibrionaceae in the environment, from the genus to the population level. *Vibrio Ecology, Pathogenesis and Evolution*, 209.
- Tao, Z., Larsen, A. M., Bullard, S. A., Wright, A. C., & Arias, C. R. (2012). Prevalence and population structure of *Vibrio vulnificus* on fishes from the northern Gulf of Mexico. *Applied and Environmental Microbiology*, 78, 7611-7618.
- Tilton, R. C., & Ryan, R. W., Clinical and Ecological Characteristics of *Vibrio Vulnificus* in the Northeastern United States. *Diagnostic Microbiology and Infectious Disease*, vol. 6, no. 2, 1987, pp. 109–117., doi:10.1016/0732-8893(87)90094-0.
- Warner, E., & Oliver, J. D. (2008a). Multiplex PCR assay for detection and simultaneous differentiation of genotypes of *Vibrio vulnificus* biotype 1. *Foodborne Pathogens and Disease*, 5, 691-693.
- Warner, E., & Oliver, J. D. (2008b). Population structures of two genotypes of *Vibrio vulnificus* in oysters (*Crassostrea virginica*) and seawater. *Applied and Environmental Microbiology*, 74, 80-85.
- Weis, K. E., Hammond, R. M., Hutchinson, R., & Blackmore, C. G. M. (2011). *Vibrio* illness in Florida, 1998–2007. *Epidemiology and Infection*, 139, 591-598.
- Whitesides, M D., & Oliver, J. D., Resuscitation of *Vibrio vulnificus* from the Viable but Nonculturable State. *Applied and Environmental Microbiology* 63.3 (1996): 1002-005. Web. 22 July 2017.
- Wong, H. C., & Wang, P. Induction of Viable but Nonculturable State in *Vibrio parahaemolyticus* and its Susceptibility to Environmental Stresses. *Journal of Applied Microbiology* 96.2 (2004): 359-66. Web.

- Wright, A. C., Miceli, G. A., Landry, W. L., Christy, J. B., Watkins, W. D., & Morris, J. G. (1993). Rapid identification of *Vibrio vulnificus* on nonselective media with an alkaline phosphatase-labeled oligonucleotide probe. *Applied and Environmental Microbiology*, 59, 541-546.
- Yamazaki, K., & Esiobu, N. Environmental predictors of pathogenic vibrios in South Florida coastal waters. *Open Epidemiology J* 5 (2012): 1-4.